Last Glacial Maximum environmental conditions at Andøya, northern Norway; evidence for a northern ice-edge ecological "hotspot"

Inger G. Alsos[1], Per Sjögren[1], Antony G. Brown[1,2], Ludovic Gielly[3], Marie Kristine Føreid Merkel[1], Aage Paus[4,5] , Youri Lammers[1], Mary E. Edwards[1,2], Torbjørn Alm[1], Melanie Leng[6], Tomasz Goslar[7], Catherine T. Langdon[2], Jostein Bakke[5,8], Willem G.M. van der Bilt[5,8]

1) UiT – The Arctic University of Norway, Tromsø Museum, N-9037 Tromsø, Norway
2) University of Southampton, Geography and Environmental Science, Southampton, SO17 1BJ, UK
3) Laboratoire d'Ecologie Alpine (LECA), Université Grenoble Alpes, C2 40700 38058, Grenoble, Cedex 9, France
4) University of Bergen, Department of Biological Science, N-5020 Bergen Norway
5) The Bjerknes Centre for Climate Research, Bergen, Norway
6) British Geological Survey, Centre for Environmental Geochemistry, Nottingham, NG12 5GG, UK
7) Faculty of Physics, Adam Mickiewicz University, Poznan, Poland
8) University of Bergen, Department of Earth Science, N-5020 Bergen, Norway

Highlights

- High organic content of Last Glacial Maximum sediments from a northern refugium.
- Isotopes and bones indicate birds roosted near the ice edge.
- Conifer DNA found in sediments, but frequency not significantly above background contamination.
- Review of all Andøya LGM studies reveals presence of boreal and arctic taxa.
- Environmental reconstruction does not preclude intermittent growth conditions for trees.
- Currently a non-analogue situation but could presage future conditions further north.

Abstract

Andøya on the NW coast of Norway is a key site for understanding the Last Glacial Maximum (LGM) in northern Europe. Controversy has arisen concerning the local conditions, especially about the timing and extent of local glacial cover, maximum July temperatures and whether pine and/or spruce could have grown there. We reviewed all existing data and add newly analysed ancient sedimentary DNA (*seda*DNA), pollen, macrofossils, geochemistry and stable isotopes from three lake sediment cores from Øvre Æråsvatnet. A total of 23 new dates and age-depth modelling suggests the lake has been ice-free since GI2 (<22.8 cal. ka BP) and possibly GS3 (<27.4 cal. ka BP). *Pinus* and *Picea seda*DNA was found in all three cores but at such low frequencies that it could not be distinguished from background contamination. LGM samples have an exceptionally high organic matter content, with isotopic values indicating that carbon and nitrogen derive from a marine source. Along with finds of bones of the little auk (*Alle alle*), this indicates that the lake received guano from an adjacent bird colony. *Seda*DNA, pollen and macrofossil assemblages were dominated by Poaceae, Brassicaceae and *Papaver*, but scattered occurrence of species currently restricted to the Low Arctic Tundra Zone (July temperature of 8-9°C) such as Apiaceae (*seda*DNA, 8-9°C), and *Alchemilla alpina* (macrofossil, 8-9°C) were also recorded. The review of >14.7 cal. ka BP data recorded 94 vascular plant taxa, of which 38% have a northern limit in Shrub Tundra or more southern vegetation zones. This unusual assemblage likely stems from a combination of proximity to ice-free water in summer, geographical isolation linked with stochastic long-distance dispersal events, and the presence of bird-fertilized habitats. The environmental reconstruction based on all records from the area does not preclude local growth of tree species, as the local climate combined with high nutrient input may have led to periodically suitable environmental 'hotspot' conditions.

Key words: ancient DNA (*a*DNA), Andøya, climate variability, environmental conditions, glacial survival, last glacial maximum, late Weichselian, MIS2, micro-refugia, sedimentary DNA (*sed*DNA)

1. Introduction

Evidence for cryptic glacial-age refugia, or micro-refugia, in the northern hemisphere has long been sought but remains elusive (Birks and Willis, 2008; Brochmann et al., 2003; Stewart and Lister, 2001; Tzedakis et al., 2013), despite the fact that phylogenetic data strongly suggest they may have existed (Anderson et al., 2006; Napier et al. 2020; Westergaard et al., 2019). It is likely that late-glacial tundra zones supported small populations of boreal trees in Alaska (Brubaker et al., 2005), Yukon (Zazula et al., 2006), Siberia (Binney et al., 2009; Tarasov et al., 2009), and Estonia (Heikkilä et al., 2009). It remains highly controversial, however, whether tree taxa grew within the maximum limits of the Scandinavian ice sheet (Birks et al., 2005; Kullman, 2005), as is indicated by megafossils of spruce and pine in the Scandinavian mountains (Kullman, 2002), and sedimentary ancient DNA (*seda*DNA) in lake sediments from a glacial refugium at Andøya (Birks et al., 2012; Parducci et al., 2012a; Parducci et al., 2012b). As all proxies for reconstructing past flora and environmental conditions have some uncertainties, a multi-proxy study may provide more robust conclusions. Environmental reconstructions are often focused on temperature (Birks and Birks, 2014; Trondman et al., 2015), but temperature may interact with other key drivers, such as nutrient cycling: high nutrient levels may compensate for low temperature, as seen, for example, at high-latitude bird cliffs (González-Bergonzoni et al., 2017). Thus, estimation of nutrient availability and trophic status may further elucidate the environmental conditions in refugia and may be critical for micro-refugia.

The northern Norwegian island of Andøya is a key locality for understanding LGM environments (here defined as the 26-18 cal. ka BP interval) on the North Atlantic margin (Vorren, 1978), and it has been extensively studied. Andøya is situated where the Norwegian continental shelf is at its narrowest (under 10 km). Due to calving into the deep ocean, there was no possibility of thick ice build-up, and the area became deglaciated early (Hughes et al., 2016; Patton et al., 2017). While higher elevations on northern parts of Andøya remained ice-free throughout the LGM (Nesje et al., 2007), it is less clear whether the lowland was continuously ice-free from ca. 26 ca. ka BP (Alm, 1993; Vorren and Plassen, 2002; Vorren et al., 2013, 2015).

Palaeobotanical investigations have been carried out on three lakes on the northern ice-free tip of Andøya (Fig. 1): Endletvatn (Alm and Elverland, 2012; Elverland, 2012; Elverland and

Alm, 2012; Parducci et al., 2012b; Vorren, 1978; Vorren and Alm, 1999, Vorren et al., 2013), Nedre Æråsvatnet (Alm and Birks, 1991; Vorren et al., 1988) and Øvre Æråsvatnet (Alm, 1993). The late-glacial vegetation recorded as pollen and plant macrofossils, combined with slow minerogenic sedimentation, has been assumed to typify cold and dry polar desert conditions (*sensu lato*). There may, however, have been interruptions: warmer periods when mean July temperatures reached up to 10°C, as indicated by features such as high concentrations/accumulation rates of pollen and/or macrofossils and the occasional presence of more thermophilous plant taxa (Alm, 1993; Alm and Birks, 1991; Elverland and Alm, 2012; Vorren, 1978). Recently, *seda*DNA of pine and spruce of LGM age was found (Parducci et al., 2012b). The discovery of conifer *seda*DNA on Andøya was unexpected, and it was debated as to whether the origin was due to contamination, long-distance pollen, driftwood, re-sedimentation, or possibly in-situ growth (Birks et al., 2012; Parducci et al., 2012a; Parducci et al., 2012b). The debate was further stirred by Vorren *et al.* (2013) who, based on both new and re-interpreted data, concluded that LGM mean July temperatures never exceeded 3°C. This interpretation would preclude any tree growth during the LGM on Andøya, but it is primarily based on the inference that the combination of the dominant moss species *Syntrichia ruralis* and *Aulacomnium turgidum* found as macrofossils represent Polar Desert vegetation, and it contradicts previous palaeoecological interpretations of past climatic conditions (Alm, 1993; Alm and Birks, 1991; Elverland and Alm, 2012; Parducci et al., 2012a; Parducci et al., 2012b; Vorren, 1978). It follows that the chronology, environmental conditions and palaeoecology of N Andøya warrant further clarification.

This study seeks to capitalize on recent advances in both the methodology (laboratory procedures, bioinformatics pipeline) and understanding of sedimentary ancient DNA to: **1**) more precisely date the ice-free period, **2**) evaluate the pine and spruce *seda*DNA results from Parducci et al. (2012b) by investigating a second lake on Andøya using improved methods; **3**) assess the local LGM palaeoenvironment based on additional proxy records, including stable isotopes, and **4**) review previous investigations, with special emphasis on environmental conditions and the potential for tree growth on Andøya during the LGM.

2. Regional setting

At Andøya (Fig. 1), the proximity of the continental shelf to abyssal depths (6.1 km from the coast to the top of the Andøya Canyon; (Laberg et al., 2000) limited the vertical extent of

glaciers during the Weichselian glaciation, and therefore the island was deglaciated early compared with other sites along the western seaboard (Vorren et al., 2015). This is in line with recent work on continental glaciation that suggests that topography/trough geometry had an overriding effect on glacial extent and recession rates (Small et al., 2018). The tip of Andøya is also crossed by ice-marginal deposits which Vorren and Plassen (2002) associated with the Egga I and Egga II deposits at the shelf edge; the Egga II dates to 23-22.2 cal. ka BP (Vorren et al., 2015).

Andøya's northern tip is an important site for LGM palaeoenvironmental studies because its lakes received sediment input at this time. This study targets Øvre Æråsvatnet (69°15'22''N; 16°02'03''E). The basin sits at 43 m a.s.l, a few meters above the local LGM marine limit. The lake has inlets to the W and SW and an outlet to the NE (Fig. 1). The July mean temperature is 11°C, and the February mean is -2.2°C; average annual precipitation is 1060 mm (Norwegian Metrological Institute; eKlima 2016; 1961–1990). The lake covers 20.4 ha, similar to the areas of two adjacent lakes, Nedre Æråsvatnet (20.6 ha, 34 m a.s.l.) and Endletvatn (28.6 ha, 35 m a.s.l.; Fig. 1). The lake is surrounded by birch forest and mires and there is planted spruce and pine, especially on the south-facing slope of Store Æråsen. The bedrock is entirely non-calcareous (amphibolites, hornblende and mica-gneisses, Norwegian Geological Survey Database), and the catchment size is 3.6 km^2.

3. Material and methods

3.1. Field work

Lake Øvre Ærsåsvatnet was chosen because, in contrast to Endletvatn, where conifer *sedaDNA* was previously detected (Parducci et al., 2012), it is above the marine limit and therefore less likely to have received driftwood. Fieldwork was conducted early in March 2014 when the lake was covered by ice. A north-south transect across the lake was test-cored using a Hiller sampler (And1-And7 and And9, Fig. 2). The laminated gyttja of expected LGM age (Alm, 1993) was only found in samples from the shallower, south-central part of the lake. To further assess sediment distribution and water depth, we surveyed the basin with Ground Penetrating Radar (GPR). For this purpose, we used a Malå GPR setup fitted with an unshielded 50 MHz antenna. The rough terrain antenna was dragged behind a snow scooter at constant speed (10 km/h) while traversing the lake in semi-regular grids. Following

acquisition, all data were processed in version 1.4 of the RadExplorer software package with a set of prescribed band-pass filtering, DC removal and time-zero adjustment routines. We then traced the interfaces between water, sediment and bedrock based on these optimized GPR reflections. Finally, all data were exported to ArcMap 10.4 to construct maps and models. Coring was conducted with a Geonor piston corer (110 mm diameter) and a modified Nesje corer (110 mm; (Nesje, 1992; Paus et al., 2015). Only the deepest part of the lake-sediment package was collected. A 3.46-m continuous core was retrieved with the modified Nesje-corer (And-11, 69.25579°N, 16.03517°E; 3.15 m water, total depth 11.88 m; subsequently divided in three parts). Two shorter cores taken with the Geonor corer (And-8, 3.15 m water, total depth 11.98 m, core length 1.14 m; And-10, 69.25552°N, 16.03516°E, 2.9 m water, total depth 10.16 m, core length 1.16 m) were collected 5 m west and 30 m south, respectively, from And-11 (Fig. 2).

3.2. Radiocarbon dating

The radiocarbon ages of 23 identified plant macrofossils were determined using Accelerator Mass Spectrometry at Poznan Radiocarbon Laboratory (Poz; Table 1). The bulk of the dated material consisted of bryophytes (moss stems), but seeds and leaf fragments of vascular plants were included when available. Low mass (TOC $\leq$ 0.2 mg) of many samples led to relatively large uncertainties, but this was preferred to combining more material. The values for $\delta^{13}C$ are given in Table 1 but are inaccurate due to having been measured with the AMS, and the unusually low $\delta^{13}C$ values reported for the smallest samples, were related to the extremely small amounts of carbon available for analysis. It is noticeable that all the $\delta^{13}C$ values are under -19. If the samples were contaminated with old C, or marine C, the values would be expected to be higher. The ^{14}C ages were calibrated with OxCal 4.2 (Bronk Ramsey, 2009) using IntCal13 (Reimer et al., 2013), and age-depth modelling was undertaken using Bacon v. 2.3.9.1 (Blaauw and Christen, 2011).

3.3. Geochemical analyses

Colour line-scan images with a resolution of approximately 70 µm were acquired using a Jai L-107CC 3 CCD RGB Line Scan Camera fitted on an Avaatech XRF core scanner (Fig. 3). Qualitative element-geochemical analyses were carried out with the XRF core scanner. The measurements were carried out at continuous 10-mm steps. Instrument settings were 10 kV, 1000 µA, 10 seconds count time, and no filter. Data processing was performed using WinAxil version 4.5.6. To minimize the influence of water and matrix effects (Tjallingii et al., 2007;

Weltje and Tjallingii, 2008), the results are presented as ratios of selected elements divided by the sum of the 7 most abundant elements (Ca, Cl, Fe, K, S, Si and Ti; Rhodium (Rh) not included as it is induced by the equipment). Loss-on-ignition (LOI) was analysed every 4 cm. About 10 g of sediment was dried overnight at 105°C, weighed, and then burned for four hours at 550°C. LOI was calculated as the percent dry-weight loss after burning.

Thirty samples were selected from the And-11 core for $\delta^{13}C$ and $\delta^{15}N$ analysis and determination of %C and %N. The isotope analyses were conducted in the Stable Isotope Facility at the British Geological Survey, UK. Samples for carbon isotopes were decarbonated in 5% HCl prior to analysis while a separate aliquot for nitrogen isotopes was run without pre-treatment. $\delta^{13}C$ analyses were performed by combustion in a Costech ECS4010 Elemental Analyser (EA) on-line to a VG TripleTrap (plus secondary cryogenic trap) and Optima dual-inlet mass spectrometer, with $\delta^{13}C$ values calculated to the VPDB scale using a within-run laboratory standard (BROC2) calibrated against external standards NBS-19 and NBS-22. Replicate analysis of well-mixed samples indicate an analytical precision of $\pm$ <0.1‰ (1 SD). Percent C and N analyses were run at the same time, and calibrated against an Acetanilide standard. $\delta^{15}N$ analyses were performed by combustion in a Thermo Finnigan Flash EA (1112 series) on-line to a Delta Plus XL mass spectrometer. $\delta^{15}N$ was calculated to the $\delta^{15}N$ value of air using the internal BROC2 standard calibrated against UGS40 and UGS41. Replicate analysis of well mixed samples indicated a precision of ±<0.2‰ (1 SD).

3.4 *seda*DNA analysis

The DNA analyses of these sediments proved challenging, and we repeated the whole process three times. For the first extraction, we followed the phosphate buffer extraction protocol of (Taberlet et al., 2012). While this works well for modern soil samples, we had poor results (as with other ancient samples). We then tried the PowerMax extraction kit (MO BIO Laboratories, Carlsbad, CA, USA), a method that has worked well for other sediments (Alsos et al., 2016; Clarke et al., 2019). Here, the results were also poor. We suspect that the main problem was the high organic content of the lower part of core And-11 and all of And-8 and And-10, as we have experienced similar problems with other highly organic sediments (Clarke et al., 2018). The uppermost, less organic part of core And-11 yielded reasonable results in all three analyses. For the third extraction, we used sterile plastic tools for taking 74 samples from the three cores. We extracted *seda*DNA using an adapted version of Zimmermann et al. (2017), in which we downscaled the input volume to ~0.3 g, substituted

the Qiagen PowerMax kit for the PowerSoil PowerLyzer kit, and incorporated a bead beating step following Alsos et al. (2016). We included negative controls during sampling (n=2), extraction (n=4), transferring extract from tubes to plates (n=2), PCR setup (n=2), and post-PCR (n=2), as well as a synthetic positive control (n=2), in total 14 controls. Here we only present data from the third extraction.

During this study, the dedicated ancient DNA laboratory of the Tromsø museum was moved twice between buildings and all reagents were replaced; the three runs exhibited different background contamination levels. We did detect pine (*Pinus*) and spruce (*Picea*) in all three runs, both in samples and in negative controls, but there were inconsistencies within samples.

For all three runs, the short and variable P6 loop region of the chloroplast trnL (UAA) intron (Taberlet et al., 2007) was used as diagnostic marker, following the same analysis protocol (Alsos et al., 2016; Sjögren et al., 2017), and running 8 PCR replicates on each DNA extract. The PCR replicates were pooled, cleaned and quantified with Qubit (Invitrogen™ Quant-iT™ and Qubit™ dsDNA HS Assay Kit, Thermofisher). The pools were converted into DNA libraries using a Truseq DNA PCR-free low throughout library prep kit (Illumina). The library was quantified by qPCR using the KAPA Library Quantification Kit for Illumina sequencing platforms (Roche) and a Prism 7500 Real Time PCR System (Life Technologies, Fisheries faculty, UiT). The library was normalised to a working concentration of 10 nM using the molarity calculated from qPCR adjusted for fragment size. Sequencing was on an Illumina HiSeq 2000 platform (2x150 bp, mid-output mode, dual indexing) at the Genomics Support Centre Tromsø (UiT).

All next-generation sequence data were aligned, filtered and trimmed using the OBITools software package (Boyer et al., 2016) using similar criteria as Alsos et al. (2016) and Sjögren et al. (2017). Resulting barcodes were assigned to taxa using the *ecotag* program (Yoccoz, 2012) and two independent reference datasets. One reference contained regional arctic and boreal sequences (Soininen et al., 2015; Sønstebø et al., 2010; Willerslev et al., 2014) and the other the NCBI nucleotide database (January 2018 release). The resulting identifications were merged and filtered, retaining barcode sequences if they: 1) were identified to 100% in either reference set; 2) were present in at least 3 PCR replicates from the same sample (hereafter referred to as PCR repeats); and 3) had at least 10 reads across the entire dataset. We removed the likely false positives relating to common PCR errors and food contaminants, based on

experience from the analyses of 15 other sediment cores in Tromsø Museum, as well as taxa identified above family level (Supplementary Table 1). For the last step of filtering, we looked at frequency of PCR repeats in samples compared to negative controls. There is no clear way to set the cut-off (Alsos et al., 2018; Sjögren et al., 2017), so we chose a conservative value, keeping only sequences that had an overall frequency of PCR repeats in samples at least twice as high as in that in negative controls. We present the data semi-quantitatively as the proportion of PCR repeats, excluding replicates that had no DNA.

3.5. Pollen and macrofossils

Pollen analysis was attempted on 19 samples from the And-11 core in the depth range 910-1182 cm. Residual material from *seda*DNA extraction 1 was used. As we resampled the core for *seda*DNA extraction 3, minor stratigraphic differences between pollen and *seda*DNA samples are possible. Every second or third level analysed for *seda*DNA in extraction 3 corresponds to a pollen sample, except 1038 cm, which was only analysed for pollen. Pollen samples (1 cm^3) were prepared (Palaeoecological laboratory, University of Southampton) using conventional methods (Berglund and Ralska-Jasiewiczowa, 1986) and mounted in silicon oil. Counting was undertaken by CL and AP. Identifications were based on (Fægri and Iversen, 1989) and (Moore et al., 1991), in combination with reference collections of modern material. In the two uppermost levels (910, 918 cm), the dryland pollen sums were 260 and 134; otherwise pollen sums were <100 grains, and often very low. In four samples the pollen sum was <10. However, we retained them to prevent imposing false negatives and because two of the records contained pine pollen which is a theoretical source of pine DNA.

Macrofossils were collected from 44 levels from core And-11 across the depth range 884-1181 cm. Slices ~2-cm thick were sampled every 8 cm (from half the core width, ca. 50 ml volume), and thus often between samples for *seda*DNA/pollen. If necessary, the samples were soaked in 10% sodium hydroxide (NaOH) to disperse organic material and/or sodium pyrophosphate ($Na_4P_2O_7$ * $10H_2O$) to disaggregate clay particles. The macrofossils were retrieved by gently sieving the sample using a 250-µm mesh. The herbarium and the macrofossil reference collection at Tromsø Museum were used to aid identification.

3.6 *seda*DNA, pollen and macrofossil data analyses

Initial diagrams were plotted in R studio version 1.2.5 using the rioja, vegan and ggplot2 packages. We explored zonation for three proxies using constrained incremental sum of

squares (CONISS) as implemented in ggplot2 version 3.2.1. Final diagrams were constructed using Tilia v.2.6.1 (https://www.tiliait.com/).

3.7 Review of botanical records and reconstruction of minimum July temperature

We used an indicator-species approach to estimating minimum July temperature based on a compilation of all published palaeo-records of taxa from Andøya for the period 26.7-14.7 cal. ka BP. The northern limits of vascular plants and vegetation types are closely linked to summer temperature (Karlsen and Elvebakk, 2003; Karlsen et al., 2005), and the Arctic is divided into bioclimatic zones representing mean July temperatures (Walker et al., 2005). We used the Pan-Arctic flora checklist (Elven et al., 2011) to assign species to the northernmost bioclimatic zones where they were (1) present or (2) frequent. If the palaeo-records were not determined to species level, the northernmost potential species in that taxon was used. Some taxa only identified to a higher taxonomic level were not classified, as ranges can be global (for example Poaceae). The choice of classification inevitably introduces bias, and our choices here lead to opposing biases regarding the kind of environment we reconstruct. First, at their northern limits most species have small population sizes and pollen production is typically low (Lamb and Edwards, 1988). Thus, a rare taxon has a low chance of occurring in palaeo records, whereas frequent species are more likely to be recorded (Schenk et al., 2020). Alternative (1) represents a conservative (cold) estimate of the minimum temperature (results given in Supplementary Table S2), whereas alternative (2) represents a mid-range estimate (results in main text) equivalent to "common northern distribution limit" (Schenk et al. 2020). Second, choice of the northernmost potential species in a group causes a strong bias towards more northerly, colder zones. For example, *Puccinellia* and *Ranunculus* occur in the polar desert zone although the majority of species in these genera do not reach the High Arctic (Elven et al., 2011); this classification in turn biases both alternatives towards colder environments.

4. Results

4.1. Bathymetry, chronology, lithostratigraphy and geochemical analysis

The updated bathymetry of lake Øvre Æråsen (Fig. 2) shows an irregular basin morphology with thick sediments across the shallow centre of the lake, and thin sediments in the deepest part. Given that the deepest sediments occur in a generally shallow area (an inversion of

normal sedimentation pattern), it is unlikely that sediments have been deposited by erosion and more likely that either there has been erosional incision or that this has resulted from ice in the lake and a coarse boulder-dominated moraine. Whether a moraine or not, the altitude of the basin, and its basal irregularity suggests disturbance of the basin in its early history. This is also suggested by the disturbed/tilted laminations in the basal sediments of Alm's (1993) core C.

Three new cores were taken and the most complete core (And-11, Fig. 3) is divided into 5 units, labelled U1 to U5, based on lithology (Table 2). As can be seen in Table 2, the basal unit is a silty-sandy diamicton capped by a thin sand unit (U1), as is typical for basal sediments. Above this are laminated gyttjas (U2 olive green, U3a rusty brown, and U3b olive green), which are markedly different from typical glacial clays expected for this period. Then follows a unit of light olive grey to white laminated silts (U4a), a moss layer (U4b), and then above olive brown to dark brown gyttjas (U5a and U5b). The unit U4a (olive grey to white with laminated silts) is unusual, but it is not a simple carbonate as shown by no acid reaction (discussed further in the results section). The moss layer above it of *Warnstorfia fluitans* (U4b, 985–995 cm) is also interesting as this suggests erosion into the lake of the surface or the edge of an acidic mire. From the stratigraphy there is a clear hiatus at between U2 and U3a (1089 cm), and two other potential hiatuses at 1178cm (in And11 but not And8), and possibly 995 cm (Fig. 3). The most parsimonious correlation based on the dates, LOI and the lithology is that the shorter core And-8 covers only part of U1-U3, while And-10 covers only U2 (Fig. 3). Unless otherwise stated, the results are coherent for the three cores.

The 23 ^{14}C dates, which are all on identified plant macrofossils, range from ca. 8 cal. ka BP to 26.7 cal. ka BP (Table 1). Several of the dates were acquired from small (<0.2 mg) samples, and some of these have stratigraphically inverted ages (too old: Poz-77610; or anomalously young: Poz-104684). Although the small sample quantities affected the date precision there is no correlation between date precision and age (correlation coefficient 0.35) suggesting age is not a causative factor. We constructed an age-depth model for And-11 *with and without* specifying the upper two hiatuses (the lowest hiatus had only one date below making modelling impossible)). When modelling the hiatus at 1089 cm depth in Bacon, 88% of the dates fell within the 95% range of the model, compared to 75% of the dates without the hiatus. The hiatus is estimated to cover the period ca. 17.2-16.2 cal. ka BP. Based on the combined dates of And-11 and And-8 the age interval of unit U2 can be estimated as ca. 23.2-

17.2 cal. ka BP. The addition of another hiatus at 995 cm was found not to improve or significantly alter the model. Thus, the model including a single hiatus at 1089 cm was preferred (Fig. 3). The modelled basal range and median were similar for the models, both with one hiatus (21,880-26,780, median 23,446 cal. ka BP) and without (21,828-26,732, median 23,366 yr BP). However, there are good reasons to assume that the basal date (Poz-77656, median 26.7 cal. ka BP) is accurate as it is in accordance with two bulk dates obtained by Alm (1993; T-8029A and T-8029B: 27,068-25,282 cal. yr BP and 26,069-25,541 cal. yr BP (at 2σ)). Our date on moss suggests that, contrary to Vorren et al's (2015) opinion, Alm´s pre-22.0 cal. ka BP dates cannot be dismissed just because they were bulk dates based on gyttja samples. This strongly suggests that a lake existed and the basin was (partially) deglaciated in the later part of GS-3, from ca. 26.7 cal. ka BP; the oldest sediments, however, have been disturbed.

Below the stratigraphically identified and modelled hiatus at 1089 cm, we see a scatter of dates based on moss fragments. This may be related to local reworking. Local reworking would still require a local terrestrial source, which implies a lack of glacial cover somewhere in the basin at an early date. The scattered ages, basal bathymetry, sediment depths and stratigraphic disturbance could indicate that the basin was partially covered by glacial ice from the cirque above it or possibly a palsa during GS3-GS2 (27.5-17.2 cal. ka BP), both of which are possible given the location of the site adjacent to the postulated ice marginal limits (Vorren et al., 2015). However, on balance we accept the U1 and U2 dates as reflecting largely ice free conditions through the last of the Weichselian glacial expansions (MIS3-2) on three principal grounds:

1. All except three samples used both terrestrial fragments (mostly seeds) and mosses. The mosses dated were all terrestrial or *Warnstorfia fluitans* which although semi-aquatic (mires) is not submerged and takes up C from terrestrial respiration on acidic mires. Thus the mosses will not have a hard-water error and cannot have skewed the radiocarbon ages.

2. Due to the geology (entirely non-calcareous - amphibolites, hornblende and mica-gneisses) the lake is acidic and the high $\delta^{13}C$ in the gyttja is not due to carbonate but due to micro-particulate guano (apatite and digestive derivatives/urea/lipids; see below) so the lake water would not have been high in calcium bicarbonate.

The dates agree with cosmogenic exposure dates, three of which are from the bird cliff (Store Ærasen), 270m from the edge of the lake. These are 37 ka BP, 37 Ka BP and 45 ka BP, and slightly further way (1.57 km) at Murdalen, 54 ka BP. Dates are also in line with the whole reconstruction of the Andøya -Skånland glacial transect by Nesje et al. (2007). Taken together, all these dates and the glacial reconstructions suggest that the north tip of Andøya was not ice-covered during the last glacial advance of the Weichselian.

Geochemical analyses (C, N, $\delta^{15}N$, $\delta^{13}C$ and XRF) were carried out on the And-11 core; LOI measurements were performed on all three cores. The most striking feature is the exceptionally high organic content in these MIS2 sediments from ca. 23.2 cal. ka BP onwards (Figs. 2 and 4). The geochemical analyses reveal four trends (Fig. 4). First, the organic content and associated elements (LOI, C%, N%, C/N, $\delta^{13}C$, $\delta^{15}N$, S, Cl and Ca) reach high values in unit U2 and U3 (Fig. 4). Second, all values, with exception of C/N and $\delta^{13}C$, show a distinct drop in the lower half of U3, i.e., U3a: LOI 60-70%, Figs. 2, 4, and C ~50%, Fig. 4), but organic content values remain unusually high for MIS2 sediments. Third, S, Cl and Ca co-vary with the LOI and C%, with the exception of an increase in Ca in unit U5b and a contrasting trend in K, Ti and Fe. In U1 to U4, these elements are negatively correlated with the organic content, and they are interpreted as representing material eroded from the catchment. The fourth trend is in Si. This element is also negatively correlated with the organic content, but in contrast to K, Ti and Fe, it increases markedly in U5. This likely signifies erosion of base-depleted soils (Boyle, 2007). Low LOI, and high K, Ti and Fe in U3–U4, indicate mineral soil depletion, suggesting temperatures above 0°C, at least seasonally, and some soil formation and erosion.

The unusually high $\delta^{13}C$ (-16 to -11) and $\delta^{15}N$ (18 to 22) values in units U2 and U3b (Fig. 5) indicate that the organic material is derived from a high trophic level. It is well outside the normal values for temperate, boreal or arctic lakes (Gąsiorowski and Sienkiewicz, 2013; Osburn et al., 2019; Thompson et al., 2018). Almost certainly, much of organic material is derived from sea-bird faeces (guano) and associated algal production, a suggestion originally made by Alm (1993). The C/N ratio is interpreted as reflecting preservation of this organic matter with moderately high N, prior to the Late Glacial and early Holocene.

4.3 Ancient DNA record

From 74 samples we obtained in total 22,888,821 raw reads, of which 1,707,668 reads of 45 sequences passed the initial filtering criteria of our pipeline (Supplementary Table S3). Two sequences matching *Vaccinium myrtillus/vitis-idaea* and three matching *Ranuculus reptans* were assumed homopolymer variants, and only the most frequent sequence was kept. Also two sequences matching pine (*Pinus*) were found. *Pinus1* was found in 19 samples (3.1% of the repeats of all samples) whereas *Pinus2* was only found in six PCR repeats at 894 cm depth in core And-11. The following taxa were found in negative controls after the filtering pipeline: spruce (*Picea*, one repeat in each of three negative controls from sampling and extraction), and one repeat of each of *Betula, Pinus1,* Poaceae and Brassicaceae. The frequency of PCR repeats of these taxa was lower in samples than in negative controls for *Picea* (0.83) and Brassicaceae (0.26), and these taxa were therefore excluded, whereas the frequency of *Pinus1* and *Betula* were 2.7 and 4.6 times higher in samples than in negative controls, respectively, and therefore kept in the dataset (Table S4). All 39 taxa, including negative controls, are presented in Supplementary Table S4, whereas the 37 assumed true positive taxa are included in Figs. 7-8. All taxa were found in core And-11. Cores And-8 and And-10 contained each eight taxa (Supplementary Table S4). The majority of the taxa were identified to a taxonomic level that allowed classification according to bioclimatic zones (Supplementary Table S5).

Taxonomic diversity was generally low in samples older than 12.7 cal. ka BP, with 0-5 taxa per sample, but it increased to 13-22 taxa in more recent samples. The highest read abundances were found for *Pinus, Ceratophyllum demersum, Myriophyllum alterniflorum,* Poaceae, and algae (*Nannochloropsis* spp.) (all > 90,000 reads). However, a more conservative estimate of DNA quantity is the number of PCR replicates, and here *Nannochloropsis gaditana* and *Nannochloropsis* sp. were by far the most dominant with 307 and 301 replicates, respectively, compared to 41 of *Caltha palustris,* 40 *Myriophyllum alterniflorum,* 39 Poaceae, and 37 PCR replicates of *Betula*.

4.4 Pollen record

In total, 60 pollen and spore types were identified in 19 samples (Supplementary Table S6). No pollen or spores were found in the basal diamicton; four samples in the basal zone (> 14.2 cal. ka BP) were essentially barren with dry-land pollen sums <5. The three youngest samples yielded >100 grains of pollen and spores. All total dry-land pollen spore concentration values were below 4000 grains per cm^{-3} except the two youngest, which had values of 8000 and

12,500 grains cm^{-3}. Less than 5 taxa (including ferns and fern allies) occurred in the lower zone, but up to 29 taxa occur in samples in the youngest zone. Most frequent grains/spores were Pteropsida (monolete spores, total count 496), Poaceae (303), *Betula*-tree type (mainly in Holocene samples, 165), and *Gymnocarpium dryopteris* (also in Holocene samples, 120). The only consistent and relatively abundant pollen taxon prior to 14.2 cal. ka BP was Poaceae. There was a clear increase in taxon richness from oldest to youngest sediments, whereas except for the two youngest samples, there was no clear pattern in concentration (Supplementary Table S6). In total, 46 of the 60 pollen and spore types could be classified to bioclimatic zones (Supplementary Table S5, Supplementary Fig. S1).

4.5 Macrofossil record

The 44 macrofossil samples included 503 records of 19 taxa/types of vascular plants, bryophytes, insect fragments, *Daphnia* ephippia and *Chara* oospores, with taxa mostly identified to species or genus level (raw counts in Supplementary Table S7). For the majority of samples, 0-3 taxa of vascular plants were found, with 4-6 taxa for the three youngest samples. Bryophytes were found in all samples (typically <50 fragments) and insect remains in most samples (typically >1000). Other abundant macrofossils were Poaceae (148 seeds), *Papaver* (110 seeds), and Brassicaceae (*Draba*-type; 15 seeds). There was a clear turnover in the macrofossil record from a dominance of *Papaver*, Poaceae and Brassicaceae to *Salix* and *Saxifraga* around 14.2 cal. ka BP, and subsequently to *Betula* and aquatics from 10.5 cal. ka BP onwards (Supplementary Fig. S2).

4.6 Combined vegetation zones

The CONISS analyses suggested five periods for each of *seda*DNA, pollen and macrofossils, but zone boundaries differed in age/depth (Supplementary Fig. S3). The only boundary identified in all three proxies, and also in the lithology, was at ca. 1018 cm depth (14.2 cal. ka BP, range 13.9-14.6 cal. ka BP). This is close to what is generally seen as the end of GS-2.1a (14.7 cal. ka BP, (Rasmussen et al., 2014), so we use this as a major boundary. Zonation before 14.2 cal. BP is based on few taxa in each of the records and thus not robust. Therefore, we keep this as one zone. After 14.2 cal. ka BP, there is a step-wise zonation with first a boundary in macrofossils around 12.8, pollen at 10.8 and 10.6, and then *seda*DNA at 9.6 cal. ka BP (Fig. 7). Below, we discuss the two major zones and their minor zonation. Cores And-8 and And-10 are both within zone 1.

4.7 Zone 1: 24.0-14.2 cal. ka BP (1182-1018 cm)

Taxon numbers per sample are low for all proxies (*seda*DNA 1-4, pollen 1-4, and macrofossils 2-6; Fig. 8). Of taxa present, most frequent are Poaceae, *Papaver* and Brassicaceae. Poaceae is a consistent taxon in all three proxies with relatively high concentrations of pollen and macrofossils. *Papaver* is recorded mostly as macrofossils (Fig. 7), occurring in all samples with up to 11 seeds per sample (Supplementary Table S7). Poaceae and *Papaver* are also present in And-8 and And-10 (Supplementary Tables S4). Brassicaceae (*Draba* type) occurs in ~50% of pollen and macrofossil samples, whereas the one *seda*DNA record was filtered out (see above and Supplementary Table S4). While ubiquitous as macrofossils, *seda*DNA of bryophytes were not found in this zone. This may be due to "swamping" of the *seda*DNA by algae (*Nannochloropsis* sp., *N. gaditana*, and for one sample in And-8 also *N. granulata*).

Other forbs present as *seda*DNA are Apiaceae (most likely *Angelica archangelica*), found in all three cores (few PCR repeats) and *Potamogeton* cf. *grammineus/alpinus*. Also present as single records are *Aster* sect. *Aster* (pollen), *Potentilla* (pollen), and cf. *Alchemilla alpina* (macrofossil; Fig. 7, Supplementary Tables S4, S6, and S7). Of the woody taxa, *Pinus seda*DNA occurs in three And-11 samples (Fig. 8) and in one and two samples in And-8 and And-10, respectively (Supplementary Table S4). It was also found as single grains in each of two pollen samples (Supplementary Table S6), but not the same ones as the *seda*DNA (Fig. 7). *Salix* occurs in a single *seda*DNA sample (And-10, Supplementary Table S4) and as a single pollen grain (Fig. 8) but not as macrofossils (Supplementary Table S7). Other woody taxa recorded were *Betula*-tree type (single grain), *Quercus* (single grain in two samples), and *Sorbus seda*DNA samples (one sample at about 14.4 cal. ka BP).

Insect fragments occur in all except the lowermost samples, increasing in abundance from around 15.5 cal. ka BP. From ca. 15.0 cal. ka BP, *Daphnia* ephippia rapidly become abundant (Fig. 7). Although generally eurythermal, most *Daphnia* species require a minimum water temperature of 10^{o}C (Clare, 2018). A bone attributed to little auk (*Alle alle*) was found at 1178 cm in And-8 (ca. 22.2-21.0 cal. ka BP), and a similar bird bone was found at 1004 cm in And-10. The number of *Nannochloropsis* repeats drops between 16.2-15.2 cal. ka BP, which is also when the sediments show a drop in LOI, C and N isotopes (Fig. 5-6).

4.10 Zone 2 *seda*DNA, pollen and macrofossils 14.2-8.2 cal. ka BP (1018- 850 cm)

Pinus is scattered in the *seda*DNA and pollen records, sometimes present in the same samples (Fig. 8a). *Salix* macrofossils appear from around 14.2 cal. ka BP, followed by *Salix* pollen and *seda*DNA (Fig. 8a). There are no samples analysed for pollen and macrofossils in the youngest sediments, but *Salix* remains frequent in the *seda*DNA record. Poaceae is present as *seda*DNA and pollen, but it almost disappears as a macrofossil (only single seeds in two samples after 14.2 cal. ka BP). *Papaver* and Brassicaceae (*Draba* type) almost disappear, but new forbs appear, e.g. *Artemisia, Oxyria, Ranuculus glacialis* (all as pollen), and *Saxifraga* spp. (pollen and macrofossils) (Fig. 8b). *Salix* was not identified to species, but given the other species in the assemblage, it likely represents dwarf shrubs such as *S. herbacea, S. polaris*, and/or *S. reticulata*. *Salix* is rare in bioclimatic zone A, the Polar Desert Zone (Walker et al., 2005), so conditions must have been warmer than that. Except for pine, no boreal species are recorded until 13.2 cal. ka BP, suggesting an arctic tundra until then.

From around 13.2 cal. ka BP, the pollen spectra include a few boreal forbs, such as *Rumex* and *Ranuculus acris*, and *Artemisia* is still present (common in low-arctic tundra but pollen potentially extra-regional, 1-4 grains per sample, Table S6) possibly suggesting an increase in temperature. In three samples dating to 12.9-12.7 cal. ka BP there is a short-lived appearance of several *seda*DNA bryophyte taxa, reflected also in higher abundance of bryophyte macrofossils (Fig. 8c) and a bryophyte band in the lithology (U4b; Fig. 3). Just above that, in U4a, there is a mixture of cold-adapted species such as *Potentilla, Oxyria*, and *Saxifraga* and boreal species such as *Rumex, Chenopodium* and *Galium*.

Soon after, at around 12.0 cal. ka BP, Apiaceae re-appears along with new taxa that have distributions north to the Low Arctic Tundra Zone: *Thalictrum*, Caryophyllaceae (*Arenaria* type), *Betula nana* and *Gentianella*. These changes suggest a transition to Low Arctic Tundra Zone or Shrub Tundra Zone, although we note that dwarf shrubs do not appear until around 11.5 cal. ka BP (scattered pollen) and are more common from 10.8 cal. ka BP. *Nannochloropsis* taxa show a clear drop from 14.2 cal. ka BP, with only scattered occurrences subsequently, whereas *Chara* oospores occur in every macrofossil sample from 12.2 cal. ka BP upwards, suggesting increasing water temperatures and some leaching of minerals from the bedrock.

The onset of the Holocene (11.7 cal. ka BP, green line in Fig. 8) is not very pronounced in the record as only a few new taxa occur (e.g. *Valeriana, Sedum,* scattered ferns) and diversity is still low in all three proxies. The largest increase in number of taxa is at around 10.8-10.6 cal. ka BP with a sudden jump from around 20 to 28-29 taxa in the pollen record, from 3-4 to 13-18 taxa in the *seda*DNA record, and from 1-2 to 5-6 taxa in the macrofossil record (Supplementary Table S4). *Betula* becomes common in all three proxies, with pollen attributed to *Betula* tree type and macrofossils identified as *B. pubescens*.. At the same time, *Filipendula ulmaria* appears in all three proxies, and ferns are abundant. The assemblage suggests a tall-herb birch forest. Aquatic floristic diversity increases with the appearance of *Caltha palustris, Isoetes, Menyanthes trifoliata, Myriophyllum alterniflorum, Potamogeton* spp.*, Sparganium* and *Subularia aquatica* (Fig. 8c). *Pinus* is found scattered in both pollen and *seda*DNA, with the highest concentration around 12.1 to 10.0 cal. ka BP (Fig. 8a). *Picea* is also found in a total of 7 of the 23 *seda*DNA samples in the period after 14.2 cal. ka BP (Supplementary Table S4), but note that we suspect *Picea* to be false positives.

4.13 Synthesis of Andøya plant and animal record >14.7 cal. ka BP

In total, 94 vascular plant taxa have been recorded from pollen (77 taxa), macrofossil (19) and aDNA (9) studies. A megafossil of *Betula pubescens* was recorded from nearby Stavdalen (ca. 20.4 cal. ka BP, Kullman, 2006) (Supplementary Table S2, S8). The most abundant taxa, both in this and previous studies, are Poaceae, Brassicaceae and *Papaver*. Poaceae may potentially include *Bromus, Festuca, Phippsia algida* and *Puccinellia.* Brassicaceae may include *Braya*-type, *Cardamine nymannii, Cochlearia,* and *Draba*-type. Vorren (1978) notes that the pollen indicates two different taxa of *Papaver*, whereas Alm and Birks (1991) note that the variation within *Papaver* seeds falls within *P. radicatum* s.lat. While over one third of recorded taxa have a northern limit in Shrub Tundra Zone (July temperatures 10-12°C) or more southern zones, the majority of these are found only as occasional pollen types that may derive from long-distance transport. A few of these, however, occur as macrofossils and/or in *seda*DNA (Table 3, Supplementary Table S2) and are likely to have grown in-situ.

Further taxa identified during the LGM and early late glacial include caddisflies and chironomids (23.5 cal. ka BP, Øvre Æråsvatnet, (Solem and Alm, 1994), Nedre Ærsåvatn – mainly 16.9 cal. ka BP onwards (Alm and Willassen, 1993) and Endletvatn, 22-14.7 cal. ka BP (Elverland and Alm 2012), and the beetle *Diernerella filum* (ca. 18-17 and 15.5 cal. ka BP, Endletvatn, Elverland and Alm 2012). The records of taxa indicating warmer conditions

largely coincide with periods of higher pollen and macrofossil concentrations (Alm, 1993; Parducci et al., 2012a). The caddisfly *Apatania zonella* is a continental species with a distribution extending east of the LGM limit to the Urals (Fauna Europaea), although it could have survived the LGM at Andøya (Solem and Alm, 1994). *Dienerella* is cosmopolitan genus, with its current Norwegian distribution restricted to a few sites in the south and one in the north. It is associated with rotting wood and musty fruit bodies of soil fungi, but it is also found in arctic tundra (Elverland and Alm, 2012, https://www.artsdatabanken.no/). Furthermore, there are records of little auk dated ca. 20-15 cal. ka BP (Alm and Elverland, 2012), eider duck (*Somateria* sp.) ca. 17.3 cal. ka BP (Vorren et al., 1988), and stoat (*Mustela erminea*) ca. 20.1-21.4 cal. ka BP (Endletvatn, (Fjellberg, 1978), re-dated by (Vorren et al., 2013).

5. Discussion

5.1 The LGM and Glaciation of Andøya

Our new date > 26 cal. ka BP strongly supports the interpretation that the northern tip of Andøya including Øvre Æråsvannet was ice-free from ca. 26 cal. ka BP. The earliest period of sedimentation, corresponding to the later part of GS-3, is disturbed, probably due to ice and the lake's location at the glacial margin. This finding aligns with three cosmogenic dates from the adjacent ridge, Store Æråsen (105 m a.s.l., 36-45 cal. ka BP, Nesje et al., 2007; Fig. 1). Vorren et al. (2013) cite the cosmogenic data; they argue that the possibility of non-erosive, cold-based glacial ice cannot be excluded. However, our new data indicate an open lake surrounded by vegetation with a nearby bird cliff. Vorren et al. (2013) also regard the earlier pre-20 cal. ka BP dates of Alm (1993) as possibly reflecting reworking. Given our new radiocarbon dates, seven of which pre-date 20 cal. ka BP and all of which are based on macrofossils, reworking also seems unlikely. The complex bathymetry combined with disturbance of the basal sediments in Øvre Æråsvatnet prior to 16 cal. ka BP suggest ice melt within the lake, as has been observed on the floor of glaciated lakes in southern Norway (Eilertsen et al., 2016) or paraglacial disturbance (Ballantyne, 2002). A very similar pattern of scattered early dates has been observed further north at Hammerfest (Birks et al. 2012). Our dates constrain the ice at the LGM on the northern tip of Andøya to a brief period after the Ålesund Interstadial (38-35 cal. ka BP; (Mangerud et al., 1981) to 26 cal. ka BP.

Alternatively, as suggested by (Mangerud, 2003), an unglaciated refugium that included Røyken and adjacent peaks on northern Andøya persisted throughout the last glacial cycle. This also has implications for the local glacial sequence. Either the outermost Egga I moraine is earlier than ca. 26 cal. ka BP, as originally argued by Vorren and Plassen (2002), or it represents a terminal moraine of a glacier in Andfjorden, the surface of which was just below Øvre Æråsvatnet. This is possible, as the Egga I moraine lies at -240 to -250 m b.s.l. and cannot be linked to an outer moraine further to the south, due to the presence of the Andøya canyon. However, it also follows that ice depositing Egga 2 cannot have covered the lake, and the only correlative moraines on the tip of Andøya (Kjølhaug, Endleten, and off shore Bleik) are all to the east and below Øvre Æråsvatnet (Fig. 1). It therefore appears that during the LGM, a very small area of Andøya, including Øvre Æråsvatnet, was an ice-free area bounded to the north by ocean (ice or water depending on season), to the east by the edge of the ice sheet, and protected to the south and west by mountains.

Given the finds in the Sunnmøre caves of little auk, other seabirds, fox and reindeer (Larsen et al., 1987), the data now available suggest that periodically an ice-free corridor existed along the outer islands of Norway, with most areas being overrun during the LGM after 26 cal. ka BP, except a small part of northern Andøya. In addition to the proximity of the continental shelf edge, our data suggest that a large sea bird population was present; this was possibly favoured by a local polynya, as has been suggested for an apparent MIS 2 ice-free area off Svalbard (van der Bilt and Lane, 2019).

5.2 Does DNA of pine and spruce derive from locally growing trees?

As in the study of nearby lake Endletvatn (Parducci et al., 2012b), we recorded DNA of pine and spruce. For the conifer DNA in Endletvatn, local growth was suggested, but alternative sources such as driftwood, reworked older material, DNA leaching, or a pollen origin were also discussed (Birks et al., 2012; Parducci et al., 2012a; Parducci et al., 2012b). Later studies indicate that DNA leaching is not a problem (Clarke et al., 2019; Sjögren et al., 2017). This is supported by the Øvre Æråsvatnet data, where virtually none of the many taxa observed in Holocene levels was recorded in samples older than 14.2 cal. ka BP (Fig. 8). Similarly, pollen is an unlikely source of chloroplast *seda*DNA (Niemeyer et al., 2017; Parducci et al., 2017; Sjögren et al., 2017), but there is less empirical evidence showing this for gymnosperms, which have paternally inherited chloroplasts. As only a few pine pollen grains were found, and these occurred in *seda*DNA samples in which no pine pollen was identified, pollen is not

a likely source of pine and spruce DNA. The likelihood of driftwood is low at Øvre Æråsvatnet, as it sits above the local marine limit. Furthermore, if driftwood were a source of *seda*DNA, we would expect to see a higher frequency of conifer DNA around 20.5 cal. ka BP, when the nearby Endletvatn was transgressed by sea for a short period (Vorren et al., 2013; Vorren et al., 1988). In line with previous interpretation (Alm, 1993), our new dates and palaeo-record do not indicate any signs of reworked material. Thus, of all the suggested sources, we think we can rule out driftwood, pollen, leaching and reworked material. This leaves contamination or local growth as explanations.

Previously, contamination was not thought to be a source of the *seda*DNA because the result had been repeated in two sediment cores and three independent laboratories (Parducci et al., 2012a; Parducci et al., 2012b). Methodology has advanced, and we have improved all parts of the methodology (extraction protocol, negative controls at all steps, running eight rather than one PCR, unique tagging to minimize tag jumps, sequencing, and bioinformatics). Nevertheless, for low-frequency sequences, it is often impossible to distinguish between true and false positives (Alsos et al., 2018; Ficetola et al., 2015; Zinger et al., 2019). When comparing modern *seda*DNA with local vegetation, a trade-off exists between retaining the true positive (i.e., true, according to the vegetation surveys) and removal of the false positives. In a recent such study, strict cut-off levels that removed the majority of false positives also removed 33% of the true positives (Alsos et al., 2018).

For ancient DNA studies, the issue of true and false positives is more challenging as independent proxies are needed for their identification. In other studies, scattered *seda*DNA records have been confirmed by macrofossils, for example, *Arabis alpina* in Svalbard (Alsos et al., 2016). We tried authentication of ancient DNA via ancient damage patterns, but shotgun sequencing of two samples from Lake Øvre Æråsvatnet did not identify sufficient pine and spruce for ancient DNA damage pattern analysis (Lammers et al. 2020).

Pine and spruce DNA are especially challenging, as they, like common food plants, can potentially be part of background contamination, due to the presence of wood or paper labels where the reagents are produced (Boessenkool et al., 2014; Clarke et al., 2018). In our laboratory at Tromsø Museum, pine and spruce were detected in 1.62% (SD=1.08, range 0-2.50%) and 1.99% (SD=2.52, range 0-6.25), respectively, of the negative control PCR repeats (n=1360 PCR repeats of 170 negative control samples), for samples processed during the

same period as this study. Thus, the frequency of pine (3.3%) is marginally above the range of background contamination in our lab, whereas the frequency of spruce (3.1%) in the three Øvre Æråsvannet samples is within that range. It is possible that even low frequencies of conifer DNA may represent true positives. Recently identified *seda*DNA in samples from the Polar Urals (ca. 21.0 and 18.0 cal. ka BP; (Clarke et al., 2019) aligns with finds of two *Picea abies* stomata dated to ca. 20.4 and 18.8 cal. ka BP (Anne Bjune pers. comm. 2019). Nevertheless, as the pine and spruce DNA record of Øvre Æråsen were not confirmed by independent proxies, and as they are within or only marginally above the background contamination, we cannot conclude anything about local presence.

As for the spruce DNA record dated to 10.3-6.3 cal. ka BP at Lake Rundtjørna, about 700 km further south (Parducci et al., 2012b), no new samples have been analysed from that region. As that study was focused on sediments that were considerably younger and closer in age to finds of megafossils in that region, there is currently no strong reason to reject the Rundtjørna spruce record.

5.3 The LGM and Late Glacial environment: a productivity hotspot?

The stable $\delta^{13}C$ /$\delta^{15}N$ values from the lower units of And-11 (U2-U3b) are highly unusual for lake sediments and indicate a marine nutrient source and high trophic level. Little auk bones were found within the enriched sediments and also at Endletvatn (ca. 20-15 cal. ka BP, Elverland and Alm 2012), along with bones of eider duck (*Somateria* sp.) at ca. 17.3 cal. ka BP (Vorren et al., 1988). The presence of ground-nesting birds is further supported by the discovery of bones of stoat (*Mustela erminea*) at Endletvatn in the interval 20.1-21.4 cal. ka BP (Fjellberg, 1978, re-dated by Vorren et al., 2013). Profundal sediments from high-arctic lakes in NW Greenland affected by marine-derived nutrients from little auk colonies show a 10-fold increase in $\delta^{15}N$ values over other sites ($\delta^{15}N$ 20.7 ± 2.4 SD), together with values for aquatic moss of 17.3 ± 5.8 and benthic algae of 17.9 ± 8.8 (González-Bergonzoni et al., 2017); these are similar to the $\delta^{15}N$ values of unit U2 (23.2-17.2 cal. ka BP.) and unit U3b (15.1-14.2 cal. ka BP) at Øvre Æråsvatnet. The Andøya data strongly suggest presence of a substantial sea-bird colony, and it is likely the lake and its surroundings were heavily manured. Furthermore, the bryophyte *Syntrichia ruralis* prefers alkaline substrates and high nitrogen (Vorren et al., 2013, http://www.arcticatlas.org). It has been estimated that marine-derived nutrients from little auk colonies underpin more than 85% of terrestrial and aquatic biomass in affected areas (González-Bergonzoni et al., 2017). Such an increase in nutrient

input would also greatly increase primary production, which fits with the unusually high organic content of the sediments for LGM and the dominance of the algae *Nannochloropsis* in the *sedaDNA* record.

Our *sedaDNA*, pollen and macrofossil record for the period 24-14.2 cal. ka BP is relatively species-poor and dominated by very few taxa (Poaceae, Brassicaceae, and *Papaver*). Neither fossil pollen assemblages nor modern plant communities provide close analogues. The modern Arctic vegetation unit B1 (cryptogam-herb barren) of the Circumpolar Arctic vegetation map (Walker et al., 2005) is most similar, but fossil pollen, *sedaDNA* and macrofossil records from the northernmost bioclimatic zones show a diversity in the flora rather than dominance by these three taxa (e.g. (Alsos et al., 2016; Bennike, 1999; Bennike and Hedenäs, 1995; Birks, 1991; Hyvärinen, 1970). In our records, the high abundance of *Papaver* probably reflects a lack of competition (Modin, 2016) combined with the availability of favourable habitats, such as screes and gravel bed channels. In the modern Arctic, high values of Brassicaceae pollen are found in association with bird-manured soils (Rozema et al., 2006; van der Knaap, 1988). Given convincing evidence of a bird colony, bird–manured arctic vegetation, combined with disturbed ground habitats in other parts of the catchment, maybe the best descriptor to the LGM vegetation on Andøya.

The four phases of warmer temperature that have been observed in previous studies (Table 3, (Alm, 1993; Alm and Birks, 1991; Elverland and Alm, 2012; Vorren et al., 2013; Vorren et al., 1988), are not pronounced in the current record (Fig. 7). The lack of signal may relate to the unusual situation of the lake. The high percentages of algal *sedaDNA* likely masked DNA of terrestrial taxa, as has been inferred from modern studies (Alsos et al., 2018). Pollen abundance in many LGM records was so low that extended counting would have yielded little information; pollen is extremely diluted by the high lacustrine productivity, and this problem applies to macrofossil counts also.

If we assume that the DNA records of *Picea* and *Pinus* are due to contamination and that pollen of *Betula* and *Quercus* is exotic, the only thermophilic species prior to 16 cal. ka BP in the current record is Apiaceae. The sequence has 100% match to several species of *Angelica* and *Heracleum*, as well as *Conioselinum tataricum* and *Podistera macounii*. Based on current biogeography and northern limits of these taxa, the sequence most likely represents *Angelica archangelica*, a species that can reach high abundances along bird cliffs today (Grønlie, 1948)

and that has its current northernmost limit in the Low Arctic Tundra (8-9°C July temperature) where it is frequent (Elven et al., 2011). The occurrence of Apiaceae is within the Andøya thermomer 2 (22–20 cal. ka BP; Table 3), concurrent with the Endletvatn *seda*DNA record (Parducci et al., 2012b), and within the period of high nitrogen and carbon isotope values (Figs. 4-5). This interval provides the strongest evidence of climate amelioration: the occurrence of several macrofossils with thermal limit at around 8°C (Elverland and Alm, 2012; Kullman, 2006; Vorren, 1978) plus *Urtica dioica,* which is rare in the Shrub Tundra (10-12°C) and common in the Boreal Zone (Elven et al., 2011; Parducci et al., 2012b).

A few more thermophilic taxa occur in our record from 15.8-14.2 cal. ka BP. We note that these are species that are either common beneath bird cliffs (e.g. *Alchemilla alpina, Angelica archangelica*) and/or easily dispersed by birds (*Potamogeton, Sorbus aucuparia*). They occur in lithological unit U3b, which is rich in nitrogen and carbon (Figs. 4-5). Both *Sorbus aucuparia* and *Potamogeton* are common north to the boreal zone (>12°C) and have scattered occurrence in Shrub Tundra (10-12°C). For this period, Vorren (1978) inferred an oceanic climate with a temperature above 10° based on macrofossils of *Sphagnum papillosum* and pollen of Apiaceae and cf. *Melampyrium*, an observation he later disregarded as likely contamination or reworked material (Vorren et al., 2013). A cold period ca 16.6-17.5 cal. ka BP, in which Vorren et al. (2013) recorded high frequencies of the arctic/alpine bryophyte *Aulacomnium turgidum*, falls within the hiatus in our core. Our core may therefore not cover the coldest period. However, the earlier record of Apiaceae pollen (Vorren, 1978) was confirmed by our Apiaceae *seda*DNA. Overall, our data and review of previous records strongly suggest at least shorter periods with July temperatures up to 10°C.

High nutrient input from birds may compensate for low temperatures (González-Bergonzoni et al., 2017). In addition, the southeast-facing slope of Store Æråsen, which is the closest likely site for such a bird cliff (Fig. 2), could have provided favourable microclimate, as south-facing slopes maximize sun exposure in the Arctic (Armbruster et al., 2007). Many bird cliffs in the Arctic today are south-facing, highly productive environments with rare species (svalbardflora.no). In addition, birds may also facilitate long-distance dispersal (Alsos et al., 2015). Thus, the combination of south-facing slope, nutrient input, and bird dispersal may have facilitated the presence of unusual (azonal) plant assemblages and allowed plants to grow beyond their normal temperature limit.

Picea and *Pinus* are currently scattered and rare, respectively, in Shrub Tundra (10-12°C) (Elven et al., 2011). *Picea abies* has been reported to survive and occasionally even to produce viable seeds at mean July-August temperatures down to 5°C (Kullman, 2002) and seeds of both *Pinus sylvestris* and *Picea abies* germinate, and may even have increased seedling survival, above the current treeline (Bougnounou et al., 2018). Recent studies have shown that nutrient availability interacts with temperature to enhance *Picea glauca* growth at the treeline in Alaska (Sullivan, 2016) and at a micro-scale to favour germination (Sullivan and Sveinbjörnsson, 2010). Thus, nutrient-rich, south-facing slopes, cliffs providing wind protection, and enhanced summer degree-day sums related to local topography, could have been relatively favourable localities for tree establishment and growth, at least during the warmest phases of LGM. Therefore, the environmental conditions based on all available evidence do not exclude local growth of *Picea* and *Pinus*, at least during short warm phases, whereas *in situ* survival during the entire LGM seems unlikely (except potentially as seeds in frozen ground).

5.4 Enrichment of the flora from 14.2 cal. ka BP

A change in flora around 14.2 cal. ka BP, with an increase in taxa as e.g. *Oxyria*, has also been observed in records from the neighbouring lakes (Vorren, 1978; Vorren et al., 1988; Alm and Birks 1991) and is associated with a change from high arctic to middle or low arctic condition (Alm 1993 and references therein).

We observed only a minor change at the onset of the Holocene (11.7 cal. ka BP), whereas the flora indicate major warming from 10.8-10.6. While Øvre Æråsen and neighbouring lakes have been intensively studied for the Full and Late Glacial period, they barely include the Holocene and sample sizes/age-depth models are poor for the transition period. Also, the nearby lake Lusvatn to the south has contaminated sediments at the transition to Holocene (Aarnes et al., 2012; Birks et al., 2014), so it is difficult to make detailed comparison. Nevertheless, the chemostratigraphc data of lake Endletvatnet indicate that the major transition was at 10.5 cal. ka BP (Vorren and Alm, 1999), corresponding to our transition for U5a to U5b at 10.6 cal. ka BP. Also, available records indicate a transition to birch forest with tall forbs and ferns (Vorren 1978; Alm 1993; Birks et al., 2014). The *seda*DNA record is especially rich in aquatic macrophytes and spore plants, including taxa not recorded in previous pollen or macrofossil records. Moreover, while some taxa appear at about the same time in all proxies e.g. *Filipendula* and *Potamogeton*, we note that they suggest slightly

different first arrival time for some key taxa such as *Salix*, *Betula* and *Vaccinium*, emphasising the advantage of using several proxies for past species distribution.

5.5 Glacial survival of plant taxa on Andøya

The presence of a *Papaver* seed in the lowermost sampled diamicton (ca. 26.7 cal. ka BP) indicates that *Papaver* may have survived the last glaciation *in situ*, supporting the conclusion of Alm and Birks (1991) for *Papaver radicatum*. This is a genetically diverse genus, and the existence of a separate genetic group of *P. radicatum* in northern Norway (Solstad, 2009) also supports the glacial survival hypothesis (Brochmann et al., 2003). That hardy taxa such as *Papaver* could have persisted through both cold and warmer phases of the last glacial period on Andøya is not particularly controversial. Other arctic or low arctic species may have survived dormant as seeds or other propagules frozen in the ground, which is also a form of survival. The scattered record of more thermophilous plant species both in this and in previous records, may indicate short-term presence, which seems more likely now that we understand the high nutrient conditions supplied by the bird cliff.

6. Conclusions

New records from three cores in Øvre Æråsvatnet confirm that northern Andøya was ice-free from at least 23.4 cal. ka BP and probably earlier (26.7 cal. ka BP), as previously suggested by Alm (1993). Local conditions were ideal for populations of cliff-nesting seabirds. This is reflected in the Øvre Æråsvatnet stratigraphy and most clearly in stable isotope values, along with further discoveries of auk bones. The presence of thermophilous taxa in *seda*DNA and macrofossils indicate at least short periods of Low Arctic Tundra conditions (July mean up to 8-9°C) and possibly Shrub Tundra conditions (July mean 10-12°C) in the period 24-14.2 cal. ka BP. We did record *Pinus* and *Picea* DNA, but the frequency was so low that it could not be distinguished from background contamination. Several recorded species have climate limits similar to those of *Pinus* and *Picea*. Based on this, and the local high-nutrient input, we conclude that environmental conditions, at least temporarily, would not exclude growth of pine and spruce, but we can provide no firm evidence for this. It is clear that in northern Andøya a combination of proximity to warm oceanic water, coastal nunataks and a sea-bird colony produced an environmental ‘hotspot’ and micro-refugia, at the edge of the Eurasian Ice sheet. This hotspot is unlikely to have been unique. While such environmental analogues

do not occur today near the edge of ice sheets, these conditions may be realized in the near future with rapid ice-sheet retreat, ecological range changes and human-aided plant dispersal.

Acknowledgements

We thank Sandra Garces Pastor for help with the *seda*DNA analyses of run 3, Arve Elvebakk for identification of a macrofossil as *Warnstorfia fluitans*, and Charlotte Clarke and Lyn Aspden for help with figures. We thank John Lowe and an anonymous reviewer for helpful comments on the manuscript. The work was supported by the Research Council of Norway (grant nos. 213692/F20, 230617/E10 and 250963/F20) and European Research Council (ERC) under the European Union's Horizon 2020 research and innovation programme (grant agreement no. 819192) to Alsos.

Author contributions

IGA, MEE and TA planned and designed the research; IGA, AP, LG and PS carried out the coring; JB and WGMB did the bathymetry; LG, IGA, MKFM and PS performed the *seda*DNA analysis; YL performed the bioinformatics analyses; AP and CTL performed the pollen analysis; PS performed the macrofossil analysis; PS, ML, and AGB performed the geochemical analyses; TG performed the AMS dating; IGA and AGB did the age-depth modelling; IGA, PS and TA carried out the review; IGA, AGB and PS organized the data and wrote the manuscript with input from all co-authors.

Conflict of Interest

Ludovic Gielly is one of the co-inventors of patents related to g-h primers and the subsequent use of the P6 loop of the chloroplast *trn*L (UAA) intron for plant identification using degraded template DNA. These patents only restrict commercial applications and have no impact on the use of this locus by academic researchers

Data availability

Raw DNA reads are uploaded at Dryad (doi:10.5061/dryad.zw3r2285q). The data obtained after filtering and taxonomic assignment are available in Supplementary Table S4.

Figures

Fig. 1. A: Map of northern Eurasia with LGM ice limits (white line) and trough-mouth fans (brown fields) after Hughes et al. (2016). The location of Andøya is highlighted with a red star. **B**: The northern part of the island Andøya with surrounding region (modified from norgeskart.no). Glacial stages discussed in the text are highlighted by stippled and dashed lines. **C**: Close-up of Lake Øvre Æråsvatnet and the surrounding lakes, as well as local moraines and coastal landforms discussed in the text. Numbers mark previous investigations: 1) Alm, 1993; 2) Vorren et al., 1988; Alm and Birks, 1991; 3) Vorren, 1978; Vorren and Alm, 1999; Alm and Elverland, 2012; Elverland, 2012; Elverland and Alm, 2012; Parducci et al., 2012b; Vorren et al., 2013; Vorren and Alm 1999.

Fig. 2. Bathymetry and sediment thickness map of Lake Øvre Æråsvatnet showing also the test cores (And5-7, And9) and sediment cores (And-8, and-10 and And11).

Fig. 3. Correlations between core And-11 (main core) and the shorter cores, And-8 and And-10. The alignment is based on lithological correlation and LOI. The dates given are median cal. years BP.

Fig. 4. Age-depth model for core And-11 from Øvre Æråsvatnet, Andøya, Norway. The calibrated 14C age ranges are shown in blue. The red lines show the statistically best model based on average of the mean, and the stippled lines show the 95% confidence interval. The horizontal stippled line shows hiatus at 1089 cm depth.

Fig. 5. Sediment properties of the core And-11 from Øvre Æråsvatnet, Andøya, Norway. Lithostratigraphic units U1-U5 are marked. The data are shown on a depth scale, with the age shown for unit boundaries. Selected elements of XRF analyses are shown as a ratio with Ti except Ti which is shown as ratio to the sum of all elements. Values above the mean are shown in black. The dates given are median cal. ka BP.

Fig. 6. A bi-plot of stable isotopes of nitrogen $\delta^{15}N$ and carbon $\delta^{13}C$ in core And-11, Øvre Æråsvatnet, Andøya, Norway. The lithological units U1-U5 are marked. Note that the age of the units spans the period 24 cal. ka BP (U1) to 8 cal. ka BP (U5). Stippled line indicate age from oldest (U1) to youngest (U6) sediments.

Fig. 7. Ancient sediment DNA (*seda*DNA), pollen and macrofossils recorded in core And-11 from Øvre Æråsvatnet (Andøya, Norway) from 23.5 cal. ka BP to 14.2 cal. ka BP. *Seda*DNA data are presented as proportion out of 8 PCR repeats, macrofossils as seeds per 50 cm^{-3} and pollen and spores as grains per cm^3. Note that the x-axes are scaled according to occurrence within each taxa and proxy; *seda*DNA data are all scaled to 1. Colour codes are according to northernmost bioclimatic subzone where the taxa is frequent (see methods). The stippled lines shows lithological units (see Fig. 3).

Fig. 8. Ancient sediment DNA (*seda*DNA), pollen and macrofossils recorded in core And-11 from Øvre Æråsvatnet (Andøya, Norway) from 16 cal. ka BP to 8 cal. ka BP. *Seda*DNA data are presented as proportion out of 8 PCR repeats, macrofossils as seeds per 50 cm^{-3} and pollen and spores as grains per cm^3. Note that the x-axes are scaled according to occurrence within each taxa and proxy; *seda*DNA data are all scaled to 1. Colour codes indicate northernmost bioclimatic subzone where the taxa is frequent (see methods). The stippled lines shows lithological units (see Fig. 3). Note that the youngest pollen and macrofossil counts were 10570 and 9540 cal. ka BP, respectively. a) Trees, shrubs, dwarf shrubs and graminoids, b) forbs, and c) bryophytes, club mosses, horsetails, ferns, aquatic, algae, and others.

Supplementary Figures

Fig. S1. Pollen diagram for And-11. Taxa only occurring in the top two samples are not included to improve readability. Pollen sum and pollen concentrations refers to total dry land pollen and spore sum and concentration per cm^3, respectively.

Fig. S2. Macrofossil diagram for And-11. Macrofossils are given as concentration if not otherwise noted. Macrofossil of leaf fragments of *Salix* and *Betula* which are given as presence/absence. Insects, *Daphnia, Chara* and bryophytes are given as 1=few (1-50 fragments), 2=common (50-1000 fragments) and 3=abundant (>1000 fragments).

Fig. S3. Correlation between lithological units (Figs. 3 and 4) and zones in *seda*DNA, pollen and macrofossils according to CONISS analyses. Note that especially for the period 23.5-14.2 cal. ka BP, there are few proxy counts and therefore the ordination is not robust. The number of samples analysed in each zone are given in brackets and main taxa for each proxy and period are indicated.

971

References

Aarnes, I., Bjune, A., Birks, H., Balascio, N., Bakke, J., Blaauw, M., 2012. Vegetation responses to rapid climatic changes during the last deglaciation 13,500–8,000 years ago on southwest Andøya, arctic Norway. Veg. Hist. Archaeobot. 21, 17-35.

Alm, T., 1993. Øvre Æråsvatn – palynostratigraphy of a 22,000 to 10,000 B.P. lacustrine record on Andøya, Northern Norway. Boreas 22, 171-188.

Alm, T., Birks, H.H., 1991. Late Weichselian flora and vegetation of Andøya, Northern Norway - macrofossil (seed and fruit) evidence from Nedre Æråsvatn. Nord. J. Bot. - Section of geobotany 11, 465-476.

Alm, T., Elverland, E., 2012. A Late Weichselian *Alle alle* colony on Andøya, northern Norway - a contribution to the history of an important Arctic environment, in: Elverland, E. (Ed.), Late Weichselian to early Holocene vegetation and bird activity on Andøya, Nordland County. As evident primarily by macrofossils. Univerity of Tromsø, PhD thesis.

Alm, T., Willassen, E., 1993. Late Weichselian chironomidae stratigraphy of Nedre Æråsvatn, Andøya, northern Norway. Hydrobiologia 254, 21-32.

Alsos, I.G., Ehrich, D., Eidesen, P.B., Solstad, H., Westergaard, K.B., Schönswetter, P., Tribsch, A., Birkeland, S., Elven, R., Brochmann, C., 2015. Long-distance plant dispersal to North Atlantic islands: colonization routes and founder effect. AoB Plants 7.

Alsos, I.G., Lammers, Y., Yoccoz, N.G., Jørgensen, T., Sjögren, P., Gielly, L., Edwards, M.E., 2018. Plant DNA metabarcoding of lake sediments: How does it represent the contemporary vegetation. PLOS ONE 13, e0195403.

Alsos, I.G., Sjögren, P., Edwards, M.E., Landvik, J.Y., Gielly, L., Forwick, M., Coissac, E., Brown, A.G., Jakobsen, L.V., Føreid, M.K., Pedersen, M.W., 2016. Sedimentary ancient DNA from Lake Skartjørna, Svalbard: Assessing the resilience of arctic flora to Holocene climate change. The Holocene 26, 627-642.

Anderson, L.L., Hu, F.S., Nelson, D.M., Petit, R.J., Paige, K.N., 2006. Ice-age endurance: DNA evidence of a white spruce refugium in Alaska. Proceedings of the National Academy of Sciences 103, 12447-12450.

Armbruster, W.S., Rae, D.A., Edwards, M.E., 2007. Topographic complexity and terrestrial biotic response to high-latitude climate change: variance is as important as the mean, in: Ørbæk, J.B., Kallenborn, R., Tombre, I., Hegseth, E.N., Falk-Petersen, S., Hoel, A.H. (Eds.), Arctic Alpine Ecosystems and People in a Changing Environment. Springer Verlag, Berlin.

Ballantyne, C.K., 2002. A general model of paraglacial landscape response. The Holocene 12, 371-376.

Bennike, O., 1999. Colonisation of Greenland by plants and animals after the last ice age: a review. Polar Rec. 35, 323-336.

Bennike, O., Hedenäs, L., 1995. Early Holocene land floras and faunas from Edgeøya, Eastern Svalbard. Polar Res. 14, 205-214.

Berglund, B.E., Ralska-Jasiewiczowa, M., 1986. Handbook of Holocene palaeoecology and palaeohydrology. John Wiley & Sons Ltd., Chichester

Binney, H.A., Willis, K.J., Edwards, M.E., Bhagwat, S.A., Anderson, P.M., Andreev, A.A., Blaauw, M., Damblon, F., Haesaerts, P., Kienast, F., Kremenetski, K.V., Krivonogov, S.K., Lozhkin, A.V., MacDonald, G.M., Novenko, E.Y., Oksanen, P., Sapelko, T.V., Väliranta, M., Vazhenina, L., 2009. The distribution of late-Quaternary woody taxa in northern Eurasia: evidence from a new macrofossil database. Quat. Sci. Rev. 28, 2445-2464.

Birks, H.H., 1991. Holocene vegetational history and climatic changes in west Spitsbergen - plant macrofossils from Skardtjørna, an Arctic lake. The Holocene 1, 209-218.
Birks, H.H., Aarnes, I., Bjune, A.E., Brooks, S.J., Bakke, J., Kühl, N., Birks, H.J.B., 2014. Lateglacial and early-Holocene climate variability reconstructed from multi-proxy records on Andøya, northern Norway. Quat. Sci. Rev. 89, 108-122.
Birks, H.H., Birks, H.J.B., 2014. To what extent did changes in July temperature influence Lateglacial vegetation patterns in NW Europe? Quat. Sci. Rev. 106, 262-277.
Birks, H.H., Giesecke, T., Hewitt, G.M., Tzedakis, P.C., Bakke, J., Birks, H.J.B., 2012. Comment on "Glacial survival of boreal trees in northern Scandinavia". Science 338, 742.
Birks, H.H., Jones, V.J., Brooks, S.J., Birks, H.J.B., Telford, R.J., Juggins, S., Peglar, S.M., 2012. From cold to cool in northernmost Norway: Lateglacial and early Holocene multi-proxy environmental and climate reconstructions from Jansvatnet, Hammerfest. Quaternary Science Reviews 33: 100-120.
Birks, H.H., Larsen, E., Birks, H.J.B., 2005. Did tree-*Betula*, *Pinus* and *Picea* survive the last glaciation along the west coast of Norway? A review of the evidence, in light of Kullman (2002). J. Biogeogr. 32, 1461-1471.
Birks, H.J.B., Willis, K.J., 2008. Alpines, trees, and refugia in Europe. Plant Ecology & Diversity 1, 147-160.
Blaauw, M., Christen, J., 2011. Flexible paleoclimate age-depth models using an autoregressive gamma process. Bayesian Analysis 6, 457-474.
Boessenkool, S., McGlynn, G., Epp, L.S., Taylor, D., Pimentel, M., Gizaw, A., Nemomissa, S., Brochmann, C., Popp, M., 2014. Use of ancient sedimentary DNA as a novel conservation tool for high-altitude tropical biodiversity. Conserv. Biol. 28, 446-455.
Bougnounou, F., Hulme, P.E., Oksanen, L., Suominen, O., Olofsson, J., 2018. Role of climate and herbivory on native and alien conifer seedling recruitment at and above the Fennoscandian treeline. J. Veg. Sci.
Boyer, F., Mercier, C., Bonin, A., Le Bras, Y., Taberlet, P., Coissac, E., 2016. OBITOOLS: a unix-inspired software package for DNA metabarcoding. Mol. Ecol. Res. 16, 176-182.
Boyle, J.F., 2007. Loss of apatite caused irreversible early-Holocene lake acidification. The Holocene 17, 543-547.
Brochmann, C., Gabrielsen, T.M., Nordal, I., Landvik, J.Y., Elven, R., 2003. Glacial survival or *tabula rasa*? The history of North Atlantic biota revisited. Taxon 52, 417-450.
Bronk Ramsey, C., 2009. Bayesian analysis of radiocarbon dates. Radiocarbon 51, 337-360.
Brubaker, L.B., Anderson, P.M., Edwards, M.E., Lozhkin, A.V., 2005. Beringia as a glacial refugium for boreal trees and shrubs: new perspectives from mapped pollen data. J. Biogeogr. 32, 833-848.
Clare, J., 2018. Daphnis: An Aquarius's Guide. V. 3.2. .
Clarke, C.L., Edwards, M.E., Brown, A.G., Gielly, L., Lammers, Y., Heintzman, P.D., Ancin-Murguzur, F.J., Bråthen, K.-A., Goslar, T., Alsos, I.G., 2018. Holocene floristic diversity and richness in northeast Norway revealed by sedimentary ancient DNA (sedaDNA) and pollen. Boreas 0.
Clarke, C.L., Edwards, M.E., Gielly, L., Ehrich, D., Hughes, P.D.M., Morozova, L.M., Haflidason, H., Mangerud, J., Svendsen, J.I., Alsos, I.G., 2019. Persistence of arctic-alpine flora during 24,000 years of environmental change in the Polar Urals. Scientific Reports 9, 19613.
Eilertsen, R.S., Bøe, R., Hermanns, R., Longva, O., Dahlgren, S., 2016. Kettle holes, 'dead-ice' topography and eskers on a lake floor in Telemark, southern Norway, in: Dowdswell, J.A., Canals, M., Jakobsson, M., Todd, B.J., Dowdeswell, E.K., Hogan,

K.A. (Eds.), Atlas of submarine glacial landforms: modern, quaternary and ancient. Geological Society of London Memoirs, pp. 113-114.
Elven, R., Murray, D.F., Razzhivin, V.Y., Yurtsev, B.A., 2011. Annotated checklist of the Panarctic Flora (PAF). Vascular plants. CAFF/University of Oslo, Natural History Museum, University of Oslo.
Elverland, E., 2012. Late Weichselian to early Holocene vegetation and bird activity on Andøya, Nordland county. As evidenced primarily by macrofossils. University of Tromsø, Tromsø.
Elverland, E., Alm, T., 2012. High resolution macrofossil analyses of Late Weichselian Arctic lacustrine sediments on Andøya, northern Norway, in: Elverland, E. (Ed.), Late Weichselian to early Holocene vegetation and bird activity on Andøya, Nordland County. As evident primarily by macrofossils. Univerity of Tromsø, PhD thesis.
Ficetola, G.F., Pansu, J., Bonin, A., Coissac, E., Giguet-Covex, C., De Barba, M., Gielly, L., Lopes, C.M., Boyer, F., Pompanon, F., Rayé, G., Taberlet, P., 2015. Replication levels, false presences and the estimation of the presence/absence from eDNA metabarcoding data. Mol. Ecol. Res. 15, 543-556.
Fjellberg, A., 1978. Fragments of a Middle Weichselian fauna on Andøya, north Norway. Boreas 7, 39-39.
Fægri, K., Iversen, J., 1989. in: Fægri, K., Kaland, P.E., Krzywinski, K. (Eds.), Textbook of pollen analysis 4. Revised edition. Wiley, Chichester, p. 314.
Gąsiorowski, M., Sienkiewicz, E., 2013. The sources of carbon and nitrogen in mountain lakes and the role of human activity in their modification determined by tracking stable isotope composition. Water, Air, & Soil Pollution 224, 1498.
González-Bergonzoni, I., Johansen, K.L., Mosbech, A., Landkildehus, F., Jeppesen, E., Davidson, T.A., 2017. Small birds, big effects: the little auk (*Alle alle*) transforms high Arctic ecosystems. Proceedings of the Royal Society B: Biological Sciences 284.
Grønlie, A.M., 1948. The ornithocoprophilous vegetation of the bird-cliffs of Røst in the Lofoten islands, northern Norway. Nyt magazin for naturvidenskaberne 86, 117-243.
Heikkilä, M., Fontana, S.L., Seppä, H., 2009. Rapid Lateglacial tree population dynamics and ecosystem changes in the eastern Baltic region. J. Quat. Sci. 24, 802-815.
Hughes, A.L.C., Gyllencreutz, R., Lohne, Ø.S., Mangerud, J., Svendsen, J.I., 2016. The last Eurasian ice sheets – a chronological database and time-slice reconstruction, DATED-1. Boreas 45, 1-45.
Hyvärinen, H., 1970. Flandrian pollen diagrams from Svalbard. Geogr. Ann. 52 A, 213-222.
Karlsen, S.R., Elvebakk, A., 2003. A method using indicator plants to map local climatic variation in the Kangerlussuaq/Scoresby Sund area, East Greenland. J. Biogeogr. 30, 1469-1491.
Karlsen, S.R., Elvebakk, A., Johansen, B., 2005. A vegetation-based method to map climatic variation in the arctic-boreal transition area of Finnmark, north-easternmost Norway. J. Biogeogr. 32, 1161-1186.
Kullman, L., 2002. Boreal tree taxa in the central Scandes during the Late-Glacial: implications for Late-Quaternary forest history. J. Biogeogr. 29, 1117-1124.
Kullman, L., 2005. On the ocurrence of late-glacial trees in the Scandes. J. Biogeogr. 32, 1499-1500.
Kullman, L., 2006. Late-glacial trees from arctic coast to alpine tundra: response to Birks et al. 2005 and 2006. J. Biogeogr. 33, 377-378.
Laberg, J.S., Vorren, T.O., Dowdeswell, J.A., Kenyon, N.H., Taylor, J., 2000. The Andøya Slide and the Andøya Canyon, north-eastern Norwegian–Greenland Sea. Marine Geology 162, 259-275.

Lamb, H., Edwards, M.E., 1988. The Arctic, in: Huntley, B., Webb, T.I. (Eds.), Vegetation history. Handbook of vegetation science 7 Kluwer Academic Publishers, Dordrecht, pp. 519-555.

Lammers, Y, Heintzman, P.H., Alsos, I.G. 2020. Environmental palaeogenomic reconstruction of an Ice Age algal population. biorxiv.org. https://doi.org/10.1101/2020.04.10.035535

Larsen, E., Gulliksen, S., Lauritzen, S.-E., Lie, R., Løvlie, R., Mangerud, J., 1987. Cave stratigraphy in western Norway; multiple Weichselian glaciations and interstadial vertebrate fauna. Boreas 16, 267-292.

Mangerud, J., 2003. Ice sheet limits in Norway and on the Norwegian continental shelf, in: Ehlers, J. (Ed.), Glacial deposits in North-West Europe. A.A. Balkema, Rotterdam, pp. 61-73.

Mangerud, J., Gulliksen, S., Larsen, E., Longva, O., Miller, G.H., Sejrup, H.-P., Sønstegaard, E., 1981. A Middle Weichselain ice-free period in Western Norway: the Ålesund Interstadial. Boreas 10, 447-462.

Modin, H., 2016. Higher temperatures increase nutrient availability in the High Arctic, causing elevated competitive pressure and a decline in Papaver radicatum, Dept of Physical Geography and Ecosystem Science.

Moore, P.D., Webb, J.A., Collinson, M.E., 1991. Pollen analysis. Blackwell Scientific Publications, Oxford.

Napier, J.D., Fernandez, M.C., de Lafontaine, G., Hu, F.S., 2020. Ice-age persistence and genetic isolation of the disjunct distribution of larch in Alaska. Ecology and Evolution https://doi.org/10.1002/ece3.6031.

Nesje, A., 1992. A piston corer for lacustrine and marine sediments. Arct. Alp. Res. 24, 257-259.

Nesje, A., Dahl, S.O., Linge, H., Ballantyne, C.K., McCarroll, D., Brook, E.J., Raisbeck, G.M., Yiou, F., 2007. The surface geometry of the Last Glacial Maximum ice sheet in the Andøya-Skånland region, northern Norway, constrained by surface exposure dating and clay mineralogy. Boreas 36, 227-239.

Niemeyer, B., Epp, L.S., Stoof-Leichsenring, K.R., Pestryakova, L.A., Herzschuh, U., 2017. A comparison of sedimentary DNA and pollen from lake sediments in recording vegetation composition at the Siberian treeline. Mol. Ecol. Res. 17, e46-e62.

Osburn, C.L., Anderson, N.J., Leng, M.J., Barry, C.D., Whiteford, E.J., 2019. Stable isotopes reveal independent carbon pools across an Arctic hydro-climatic gradient: Implications for the fate of carbon in warmer and drier conditions. Limnology and Oceanography Letters 4, 205-213.

Parducci, L., Bennett, K.D., Ficetola, G.F., Alsos, I.G., Suyama, Y., Wood, J.R., Pedersen, M.W., 2017. Transley Reviews: Ancient plant DNA from lake sediments. New Phytol. 214, 924-942.

Parducci, L., Edwards, M.E., Bennett, K.D., Alm, T., Elverland, E., Tollefsrud, M.M., Jørgensen, T., Houmark-Nielsen, M., Larsen, N.K., Kjær, K.H., Fontana, S.L., Alsos, I.G., Willerslev, E., 2012a. Response to Comment on "Glacial Survival of Boreal Trees in Northern Scandinavia". Science 338, 742.

Parducci, L., Jørgensen, T., Tollefsrud, M.M., Elverland, E., Alm, T., Fontana, S.L., Bennett, K.D., Haile, J., Matetovici, I., Suyama, Y., Edwards, M.E., Andersen, K., Rasmussen, M., Boessenkool, S., Coissac, E., Brochmann, C., Taberlet, P., Houmark-Nielsen, M., Larsen, N.K., Orlando, L., Gilbert, M.T.P., Kjær, K.H., Alsos, I.G., Willerslev, E., 2012b. Glacial survival of boreal trees in northern Scandinavia. Science 335, 1083-1086.

Patton, H., Hubbard, A., Andreassen, K., Auriac, A., Whitehouse, P.L., Stroeven, A.P., Shackleton, C., Winsborrow, M., Heyman, J., Hall, A.M., 2017. Deglaciation of the Eurasian ice sheet complex. Quat. Sci. Rev. 169, 148-172.

Paus, A., Boessenkool, S., Brochmann, C., Epp, L.S., Fabel, D., Haflidason, H., Linge, H., 2015. Lake Store Finnsjøen – a key for understanding Lateglacial/early Holocene vegetation and ice sheet dynamics in the central Scandes Mountains. Quat. Sci. Rev. 121, 36-51.

Rasmussen, T.L., Thomsen, E., Skirbekk, K., Ślubowska-Woldengen, M., Klitgaard Kristensen, D., Koç, N., 2014. Spatial and temporal distribution of Holocene temperature maxima in the northern Nordic seas: interplay of Atlantic-, Arctic- and polar water masses. Quat. Sci. Rev. 92, 280-291.

Reimer, P.J., Bard, E., Bayliss, A., Beck, J.W., Blackwell, P.G., Bronk Ramsey, C., Buck, C.E., Cheng, H., Edwards, R.L., Friedrich, M., Grootes, P.M., Guilderson, T.P., Haflidason, H., Hajdas, I., Hatté, C., Heaton, T.J., Hoffmann, D.L., Hogg, A.G., Hughen, K.A., Kaiser, K.F., Kromer, B., Manning, S.W., Niu, M., Reimer, R.W., Richards, D.A., Scott, E.M., Southon, J.R., Staff, R.A., Turney, C.S.M., van der Plicht, J., 2013. IntCal13 and marine13 radiocarbon age calibration curves 0–50,000 years cal BP.

Rozema, J., Boelen, P., Doorenbosch, M., Bohncke, S., Blokker, P., Boekel, C., Broekman, R., Konert, M., 2006. A vegetation, climate and environment reconstruction based on palynological analyses of high arctic tundra peat cores (5000–6000 years BP) from Svalbard. Plants and Climate Change 41, 155-174.

Sjögren, P., Edwards, M.E., Gielly, L., Langdon, C.T., Croudace, I.W., Merkel, M.K.F., Fonville, T., Alsos, I.G., 2017. Lake sedimentary DNA accurately records 20th Century introductions of exotic conifers in Scotland. New Phytol. 213, 929-941.

Small, D., Smedley, R.K., Chiverrell, R.C., Scourse, J.D., Cofaigh, C.Ó., Duller, G.A.T., McCarron, S., Burke, M.J., Evans, D.J.A., Fabel, D., Gheorghiu, D.M., Thomas, G.S.P., Xu, S., Clark, C.D., 2018. Trough geometry was a greater influence than climate-ocean forcing in regulating retreat of the marine-based Irish-Sea Ice Stream. GSA Bulletin 130, 1981-1999.

Soininen, E.M., Gauthier, G., Bilodeau, F., Berteaux, D., Gielly, L., Taberlet, P., Gussarova, G., Bellemain, E., Hassel, K., Stenøien, H.K., Epp, L., Schrøder-Nielsen, A., Brochmann, C., Yoccoz, N.G., 2015. Highly overlapping diet in two sympatric lemming species during winter revealed by DNA metabarcoding. Plos One 10, e0115335.

Solem, J.O., Alm, T., 1994. Southwards migration of freshwater invertebrates from northern Norway. Fauna norv. Ser. A 15, 9-18.

Solstad, H., 2009. Taxonomy and evolution of the diploid and polyploid *Papaver* sect. *Meconella* (Papaveraceae), National Scentre for Biosystematics, Faculty of Mathematics and Natural Science. University of Oslo, Oslo.

Stewart, J.R., Lister, A.M., 2001. Cryptic northern refugia and the origins of the modern biota. Trends Ecol. Evol. 16, 608-613.

Sullivan, P.F., 2016. Evidence of soil nutrient availability as the proximate constraint on growth of treeline trees in northwest Alaska: reply. Ecology 97, 803-808.

Sullivan, P.F., Sveinbjörnsson, B., 2010. Microtopographic control of treeline advance in Noatak National Preserve, Northwest Alaska. Ecosystems 13, 275-285.

Sønstebø, J.H., Gielly, L., Brysting, A.K., Elven, R., Edwards, M., Haile, J., Willerslev, E., Coissac, E., Rioux, D., Sannier, J., Taberlet, P., Brochmann, C., 2010. Using next-generation sequencing for molecular reconstruction of past Arctic vegetation and climate. Mol. Ecol. Res. 10, 1009-1018.

Taberlet, P., Coissac, E., Pompanon, F., Gielly, L., Miquel, C., Valentini, A., Vermat, T., Corthier, G., Brochmann, C., Willerslev, E., 2007. Power and limitations of the chloroplast trnL (UAA) intron for plant DNA barcoding. Nucleic Acids Res. 35, e14.

Taberlet, P., Prud'Homme, S.M., Campione, E., Roy, J., Miquel, C., Shehzad, W., Gielly, L., Rioux, D., Choler, P., ClÉMent, J.-C., Melodelima, C., Pompanon, F., Coissac, E., 2012. Soil sampling and isolation of extracellular DNA from large amount of starting material suitable for metabarcoding studies. Mol. Ecol. 21, 1816-1820.

Tarasov, P., Müller, S., A. Andreev, Werner, K., Diekmann, B., 2009. Younger Dryas *Larix* in eastern Siberia: A migrant or survivor? PAGES news 17, 122-124.

Thompson, H.A., White, J.R., Pratt, L.M., 2018. Spatial variation in stable isotopic composition of organic matter of macrophytes and sediments from a small Arctic lake in west Greenland. Arct. Antarct. Alp. Res. 50, S100017.

Tjallingii, R., Röhl, U., Kölling, M., Bickert, T., 2007. Influence of the water content on X-ray fluorescence core-scanning measurements in soft marine sediments. Geochemistry, Geophysics, Geosystems 8, Q02004.

Trondman, A.K., Gaillard, M.J., Mazier, F., Sugita, S., Fyfe, R., Nielsen, A.B., Twiddle, C., Barratt, P., Birks, H.J.B., Bjune, A.E., Björkman, L., Broström, A., Caseldine, C., David, R., Dodson, J., Dörfler, W., Fischer, E., Geel, B., Giesecke, T., Hultberg, T., Kalnina, L., Kangur, M., Knaap, P., Koff, T., Kuneš, P., Lagerås, P., Latałowa, M., Lechterbeck, J., Leroyer, C., Leydet, M., Lindbladh, M., Marquer, L., Mitchell, F.J.G., Odgaard, B.V., Peglar, S.M., Persson, T., Poska, A., Rösch, M., Seppä, H., Veski, S., Wick, L., 2015. Pollen-based quantitative reconstructions of Holocene regional vegetation cover (plant-functional types and land-cover types) in Europe suitable for climate modelling. Global Change Biol. 21, 676-697.

Tzedakis, P.C., Emerson, B.C., Hewitt, G.M., 2013. Cryptic or mystic? Glacial tree refugia in northern Europe. Trends in Ecology & Evolution 28, 696-704.

van der Bilt, W.G.M., Lane, C.S., 2019. Lake sediments with Azorean tephra reveal ice-free conditions on coastal northwest Spitsbergen during the Last Glacial Maximum. Science Advances 5, eaaw5980.

van der Knaap, W.O., 1988. A pollen diagram from Brøggerhalvøya, Spitsbergen: changes in vegetation and environment from ca. 4400 to ca. 800 B.P. Arct. Alp. Res. 20, 106-116.

Vorren, K.D., 1978. Late and Middle Weichselian stratigraphyof Andøya, north Norway. Boreas 7, 19-38.

Vorren, K. D., Alm, T., 1999. "Late Weichselian and Holocene environments of lake Endlevatn, Andøya, northern Norway: as evidenced prilimarily by chemostratigraphical data." Boreas 28: 505-520.

Vorren, T.O., Plassen, L., 2002. Deglaciation and palaeoclimate of the Andfjord-Vågsfjord area, North Norway. Boreas 31, 97-125.

Vorren, T.O., Rydningen, T.A., Baeten, N.J., Laberg, J.S., 2015. Chronology and extent of the Lofoten–Vesterålen sector of the Scandinavian Ice Sheet from 26 to 16 cal. ka BP. Boreas 44, 445-458.

Vorren, T.O., Vorren, K.-D., Aasheim, O., Dahlgren, K.I.T., Forwick, M., Hassel, K., 2013. Palaeoenvironment in northern Norway between 22.2 and 14.5 cal. ka BP. Boreas, 876–895

Vorren, T.O., Vorren, K.-D., Alm, T., Gulliksen, S., Løvlie, R., 1988. The last deglaciation (20,000 - 11,000 B.P.) on Andøya, Northern Norway. Boreas 17, 41-77.

Walker, D.A., Raynolds, M.K., Daniels, F.J.A., Einarsson, E., Elvebakk, A., Gould, W.A., Katenin, A.E., Kholod, S.S., Markon, C.J., Melnikov, E.S., Moskalenko, N.G., Talbot, S.S., Yurtsev, B.A., 2005. The circumpolar arctic vegetation map. J. Veg. Sci. 16, 267-282.

Weltje, G.J., Tjallingii, R., 2008. Calibration of XRF core scanners for quantitative geochemical logging of sediment cores: Theory and application. Earth Planet. Sci. Lett. 274, 423-438.

Westergaard, K.B., Zemp, N., Bruederle, L.P., Stenøien, H.K., Widmer, A., Fior, S., 2019. Population genomic evidence for plant glacial survival in Scandinavia. Mol. Ecol. 28, 818-832.

Willerslev, E., Davison, J., Moora, M., Zobel, M., Coissac, E., Edwards, M.E., Lorenzen, E.D., Vestergard, M., Gussarova, G., Haile, J., Craine, J., Gielly, L., Boessenkool, S., Epp, L.S., Pearman, P.B., Cheddadi, R., Murray, D., Bråthen, K.A., Yoccoz, N., Binney, H., Cruaud, C., Wincker, P., Goslar, T., Alsos, I.G., Bellemain, E., Brysting, A.K., Elven, R., Sonstebo, J.H., Murton, J., Sher, A., Rasmussen, M., Ronn, R., Mourier, T., Cooper, A., Austin, J., Moller, P., Froese, D., Zazula, G., Pompanon, F., Rioux, D., Niderkorn, V., Tikhonov, A., Savvinov, G., Roberts, R.G., MacPhee, R.D.E., Gilbert, M.T.P., Kjaer, K.H., Orlando, L., Brochmann, C., Taberlet, P., 2014. Fifty thousand years of Arctic vegetation and megafaunal diet. Nature 506, 47-51.

Yoccoz, N.G., 2012. The future of environmental DNA in ecology. Mol. Ecol. 21, 2031-2038.

Zazula, G.D., Telka, A.M., Harington, C.R., Schweger, C.E., Mathewes, R.W., 2006. New Spruce (*Picea* spp.) macrofossils from Yukon Territory: implications for Late Pleistocene refugia in eastern Beringia. Arctic 59, 391-400.

Zimmermann, H.H., Raschke, E., Epp, L.S., Stoof-Leichsenring, K.R., Schwamborn, B., Schirrmeister, L., Overduin, P.P., Herzschuh, H., 2017. Sedimentary ancient DNA and pollen reveal the composition of plant organic matter in Late Quaternary permafrost sediments of the Buor Khaya Peninsula (north-eastern Siberia). Biogeosciences 14: 575-596.

Zinger, L., Bonin, A., Alsos, I.G., Bálint, M., Bik, H., Boyer, F., Chariton, A.A., Creer, S., Coissac, E., Deagle, B.E., De Barba, M., Dickie, I.A., Dumbrell, A.J., Ficetola, G.F., Fierer, N., Fumagalli, L., Gilbert, M.T.P., Jarman, S., Jumpponen, A., Kauserud, H., Orlando, L., Pansu, J., Pawlowski, J., Tedersoo, L., Thomsen, P.F., Willerslev, E., Taberlet, P., 2019. DNA metabarcoding—Need for robust experimental designs to draw sound ecological conclusions. Mol. Ecol. 28, 1857-1862.

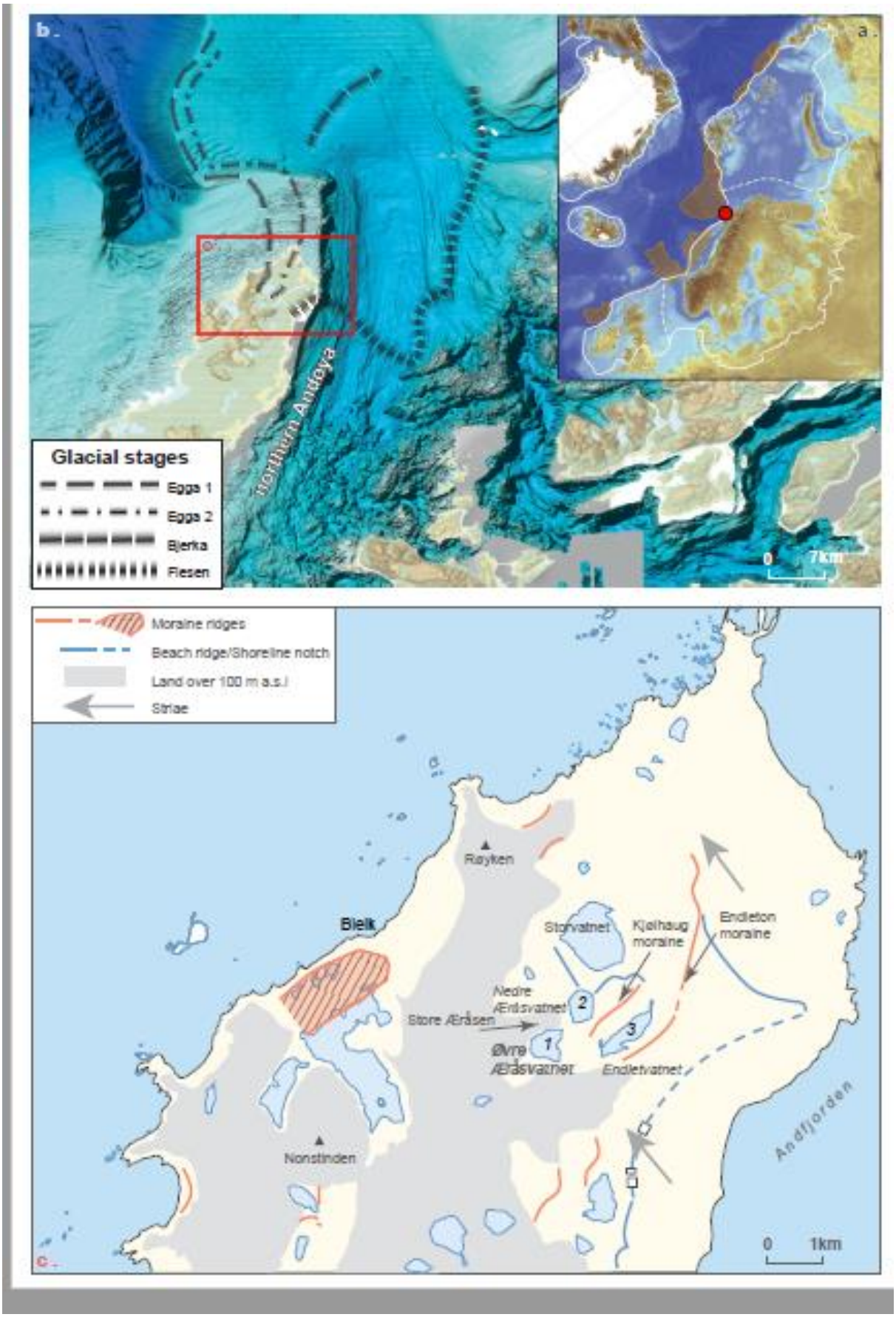
b.
a.
Glacial stages
Egga 1
Egga 2
Bjerka
Flesen
northern Andøya
0 7km
Moraine ridges
Beach ridge/Shoreline notch
Land over 100 m a.s.l.
Striae
Bleik
Røyken
Storvatnet
Kjelhaug moraine
Endleton moraine
Nedre Ærâsvatnet
Store Ærâsen
Øvre Ærâsvatnet
Endletvatnet
Nonstinden
Andfjorden
0 1km
c.

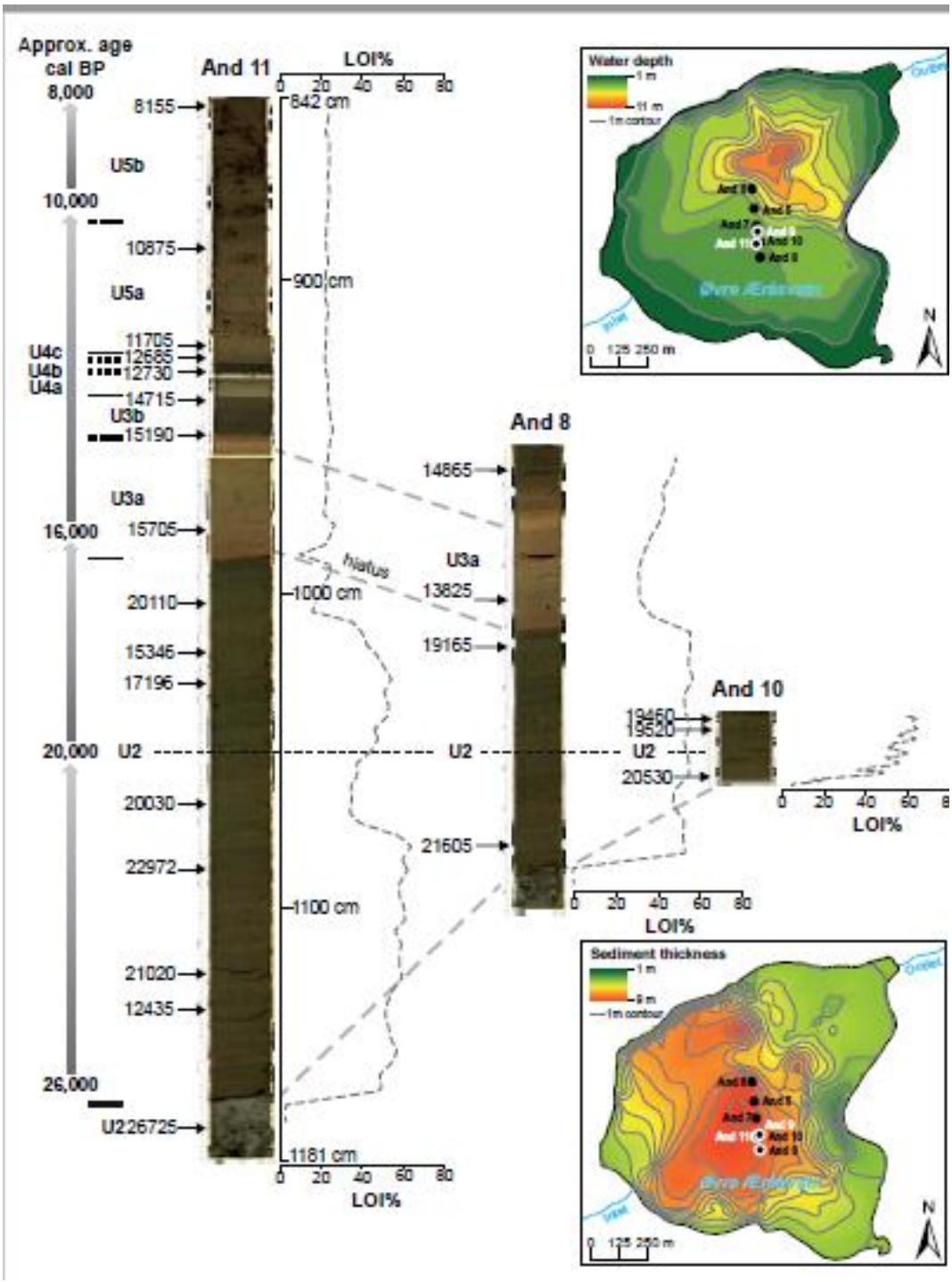
Approx. age
cal BP
8,000
10,000
16,000
20,000
26,000
And 11
LOI%
0 20 40 60 80
842 cm
900 cm
1000 cm
1100 cm
1181 cm
8155
10875
11705
12665
12730
14715
15190
15705
20110
15346
17196
20030
22972
21020
12435
U226725
U5b
U5a
U4c
U4b
U4a
U3b
U3a
U2
hiatus
And 8
14865
13825
19165
21605
And 10
19450
19520
20530
Water depth
1 m
11 m
1m contour
Outlet
And 8
And 5
And 7
And 11
And 9
And 10
And 6
Øvre Æråvatn
Inlet
0 125 250 m
N
Sediment thickness
1 m
9 m
1m contour

1302
1303

1304

And 11 Geoproxies

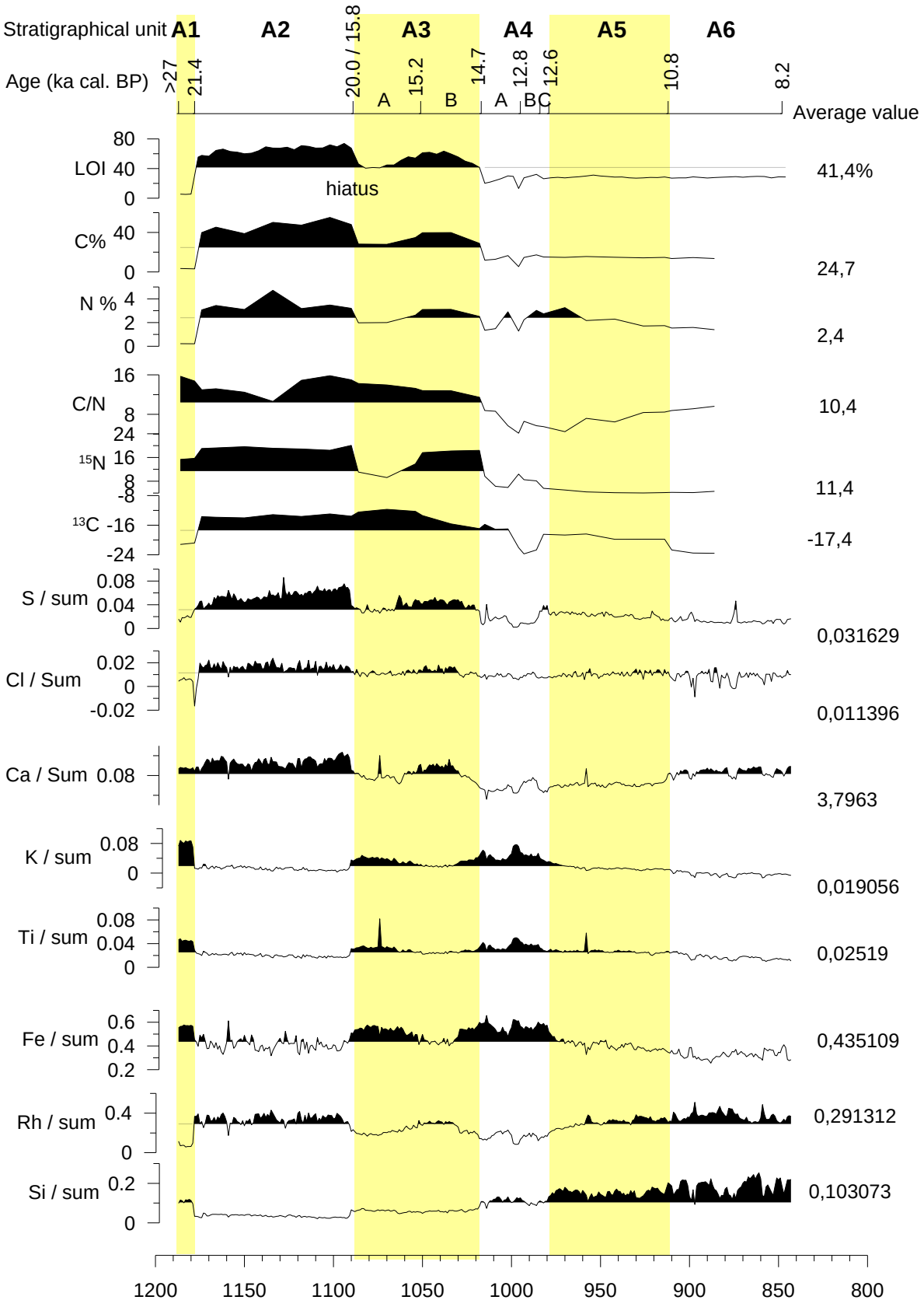

1305
1306

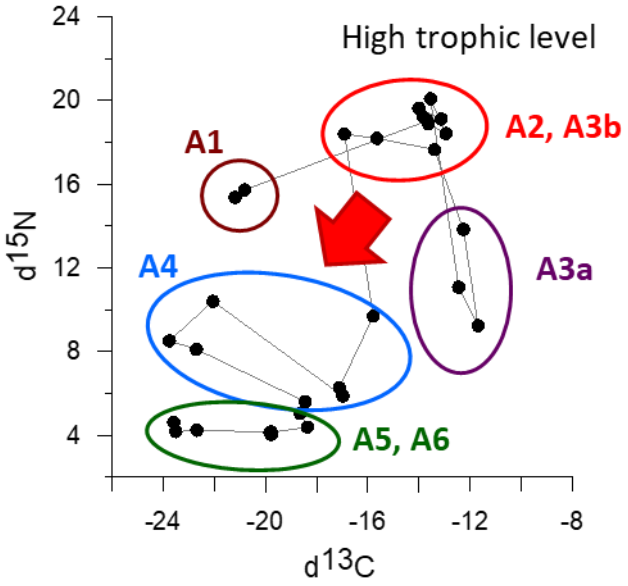
High trophic level
A1
A2, A3b
A3a
A4
A5, A6
d15N
d13C
24
20
16
12
8
4
-24
-20
-16
-12
-8

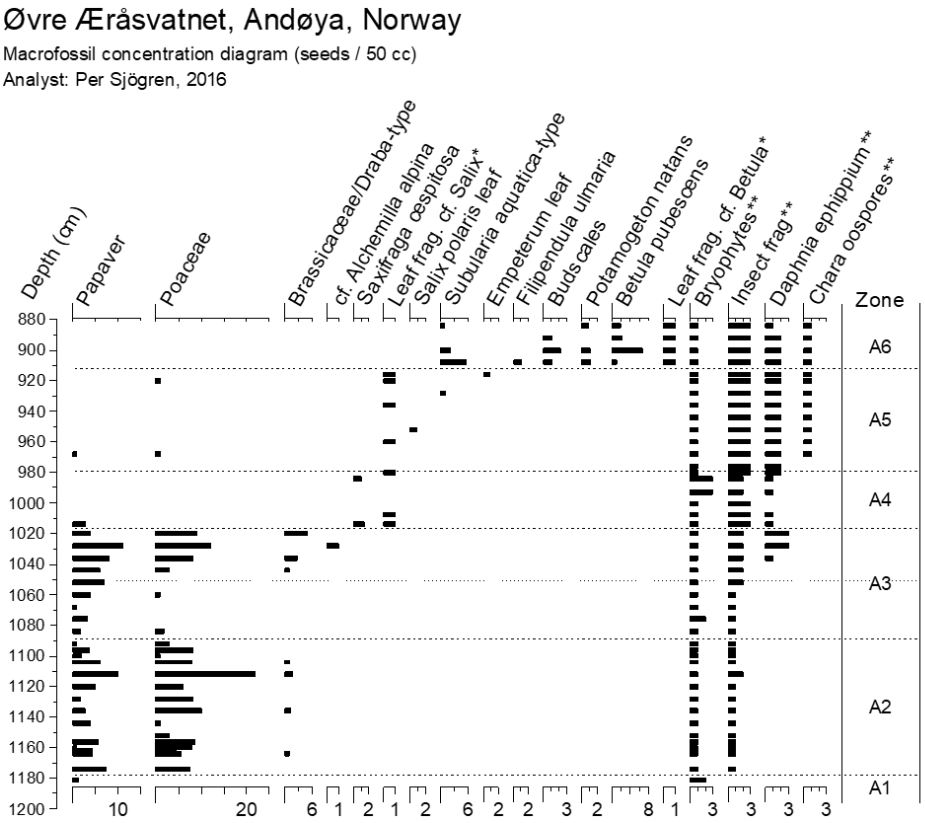
Øvre Æråsvatnet, Andøya, Norway
Macrofossil concentration diagram (seeds / 50 cc)
Analyst: Per Sjögren, 2016
Depth (cm)
Papaver
Poaceae
Brassicaceae/Draba-type
cf. Alchemilla alpina
Saxifraga oppositifolia
Leaf frag. cf. Salix*
Salix polaris leaf
Subularia aquatica-type
Empetrum leaf
Filipendula ulmaria
Budscales
Potamogeton natans
Betula pubescens
Leaf frag. cf. Betula*
Bryophytes**
Insect frag**
Daphnia ephippium**
Chara oospores**
Zone
A6
A5
A4
A3
A2
A1

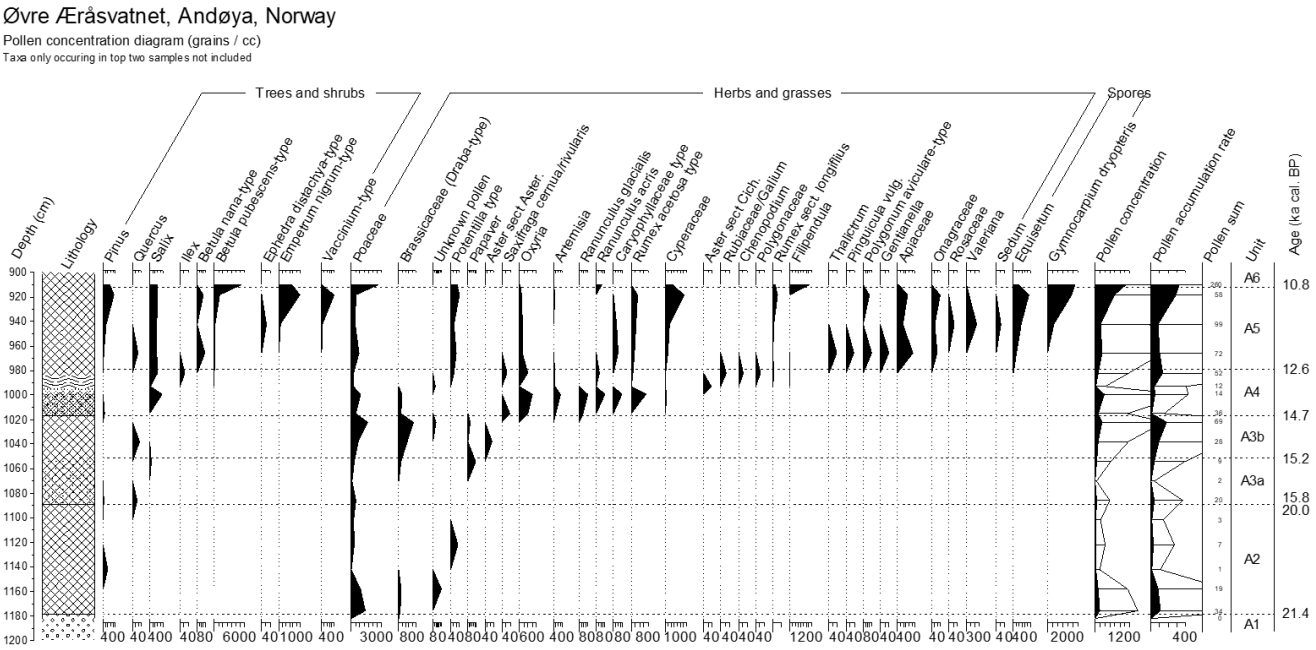
Øvre Æråsvatnet, Andøya, Norway
Pollen concentration diagram (grains / cc)
Taxa only occuring in top two samples not included
Trees and shrubs
Herbs and grasses
Spores
Depth (cm)
Lithology
Pinus
Quercus
Salix
Ilex
Betula nana-type
Betula pubescens-type
Ephedra distachya-type
Empetrum nigrum-type
Vaccinium-type
Poaceae
Brassicaceae (Draba-type)
Unknown pollen
Potentilla type
Papaver
Aster sect Aster.
Saxifraga cernua/rivularis
Oxyria
Artemisia
Ranunculus glacialis
Ranunculus acris
Caryophyllaceae type
Rumex acetosa type
Cyperaceae
Aster sect Cich.
Rubiaceae/Galium
Chenopodium
Polygonaceae
Rumex sect. longifolius
Filipendula
Thalictrum
Pinguicula vulg.
Polygonum aviculare-type
Gentianella
Apiaceae
Onagraceae
Rosaceae
Valeriana
Sedum
Equisetum
Gymnocarpium dryopteris
Pollen concentration
Pollen accumulation rate
Pollen sum
Unit
Age (ka cal. BP)
A6
A5
A4
A3b
A3a
A2
A1
10.8
12.6
14.7
15.2
15.8
20.0
21.4
Analysts: Aage Paus, Catherine Langdon

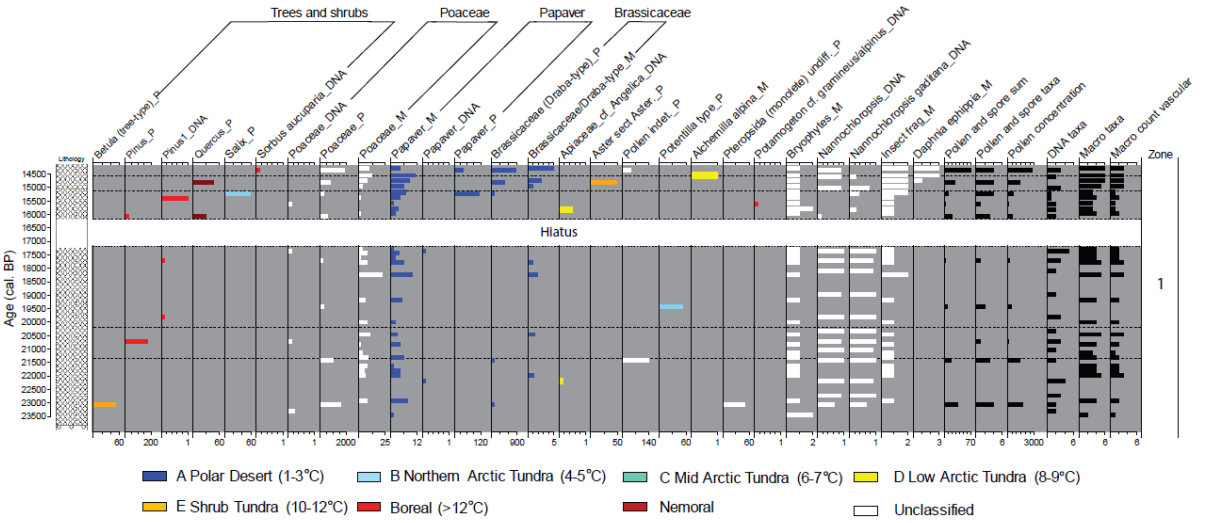
Trees and shrubs
Poaceae
Papaver
Brassicaceae
Betula (tree-type)_P
Pinus_P
Pinus1_DNA
Quercus_P
Salix_P
Sorbus aucuparia_DNA
Poaceae_DNA
Poaceae_P
Poaceae_M
Papaver_M
Papaver_DNA
Papaver_P
Brassicaceae (Draba-type)_P
Brassicaceae/Draba-type_M
Apiaceae_cf_Angelica_DNA
Aster sect Aster._P
Pollen indet._P
Potentilla type_P
Alchemilla alpina_M
Pteropsida (monolete) undiff._P
Potamogeton cf. gramineus/alpinus_DNA
Bryophytes_M
Nannochloropsis_DNA
Nannochloropsis gaditana_DNA
Insect frag_M
Daphnia ephippia_M
Pollen and spore sum
Pollen and spore taxa
Pollen concentration
DNA taxa
Macro taxa
Macro count vascular
Zone
Lithology
Age (cal. BP)
Hiatus
1
A Polar Desert (1-3°C)
B Northern Arctic Tundra (4-5°C)
C Mid Arctic Tundra (6-7°C)
D Low Arctic Tundra (8-9°C)
E Shrub Tundra (10-12°C)
Boreal (>12°C)
Nemoral
Unclassified

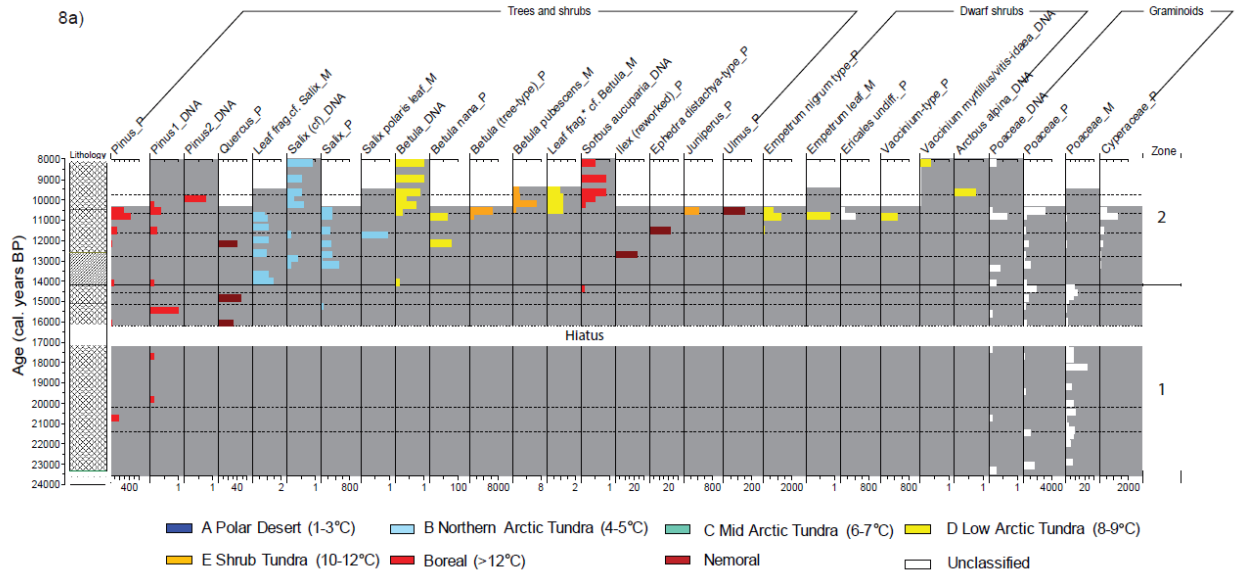
8a)
Trees and shrubs
Dwarf shrubs
Graminoids
Pinus_P
Pinus1_DNA
Pinus2_DNA
Quercus_P
Leaf frag.cf.Salix_M
Salix (cf)_DNA
Salix_P
Salix polaris leaf_M
Betula_DNA
Betula nana_P
Betula (tree-type)_P
Betula pubescens_M
Leaf frag.* cf. Betula_M
Sorbus aucuparia_DNA
Ilex (reworked)_P
Ephedra distachya-type_P
Juniperus_P
Ulmus_P
Empetrum nigrum type_P
Empetrum leaf_M
Ericales undiff._P
Vaccinium-type_P
Vaccinium myrtillus/vitis-idaea_DNA
Arctous alpina_DNA
Poaceae_DNA
Poaceae_P
Poaceae_M
Cyperaceae_P
Lithology
Zone
Age (cal. years BP)
Hiatus
A Polar Desert (1-3°C)
B Northern Arctic Tundra (4-5°C)
C Mid Arctic Tundra (6-7°C)
D Low Arctic Tundra (8-9°C)
E Shrub Tundra (10-12°C)
Boreal (>12°C)
Nemoral
Unclassified

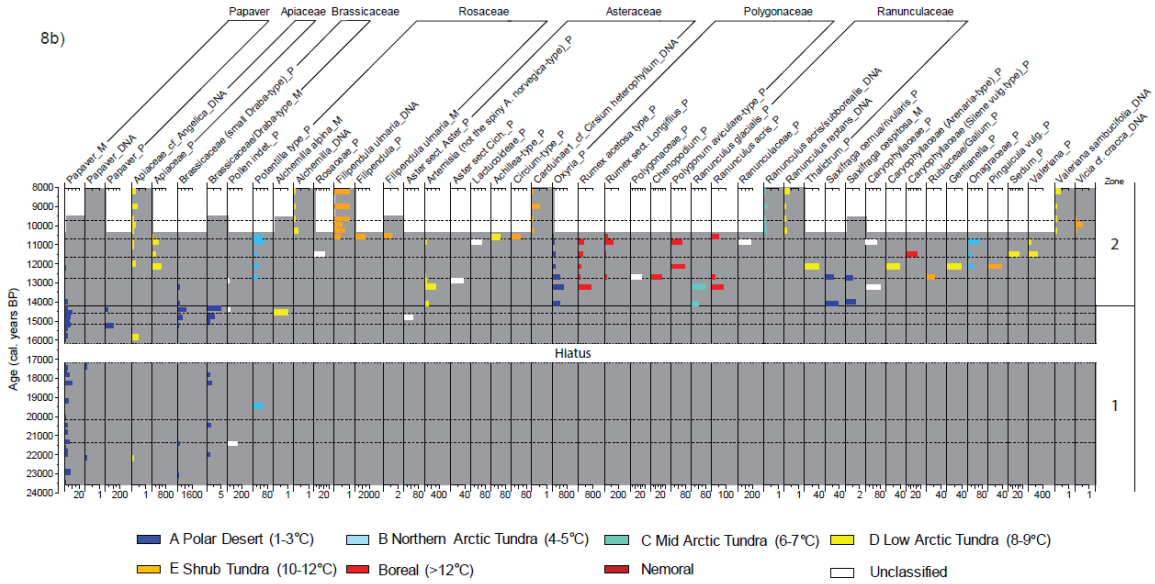
8b)
Papaver
Apiaceae
Brassicaceae
Rosaceae
Asteraceae
Polygonaceae
Ranunculaceae
Papaver_M
Papaver_DNA
Papaver_P
Apiaceae_cf_Angelica_DNA
Apiaceae_P
Brassicaceae (small Draba-type)_P
Brassicaceae/Draba-type_M
Pollen indet._P
Potentilla type_P
Alchemilla alpina_M
Alchemilla_DNA
Rosaceae_P
Filipendula_P
Filipendula ulmaria_DNA
Filipendula ulmaria_M
Aster sect. Aster_P
Artemisia (not the spiny A. norvegica-type)_P
Aster sect.Cicin._P
Lactucoideae_P
Achillea-type_P
Cirsium-type_P
Cardunae1_cf_Cirsium heterophyllum_DNA
Oxyria_P
Rumex acetosa type_P
Rumex sect. Longifolius_P
Polygonaceae_P
Chenopodium_P
Polygonum aviculare-type_P
Ranunculus glacialis_P
Ranunculus acris_P
Ranunculaceae_P
Ranunculus acris/subborealis_DNA
Thalictrum_P
Ranunculus reptans_DNA
Saxifraga cernua/nivalis_P
Saxifraga opposita_M
Caryophyllaceae_P
Caryophyllaceae_M
Caryophyllaceae (Arenaria-type)_P
Rubiaceae/Galium_P
Gentianella_P
Omalotheca_P
Pinguicula vulg._P
Sedum_P
Valeriana_P
Valeriana sambucifolia_DNA
Vicia cf. cracca_DNA
Zone
Age (cal. years BP)
Hiatus
A Polar Desert (1-3°C)
B Northern Arctic Tundra (4-5°C)
C Mid Arctic Tundra (6-7°C)
D Low Arctic Tundra (8-9°C)
E Shrub Tundra (10-12°C)
Boreal (>12°C)
Nemoral
Unclassified

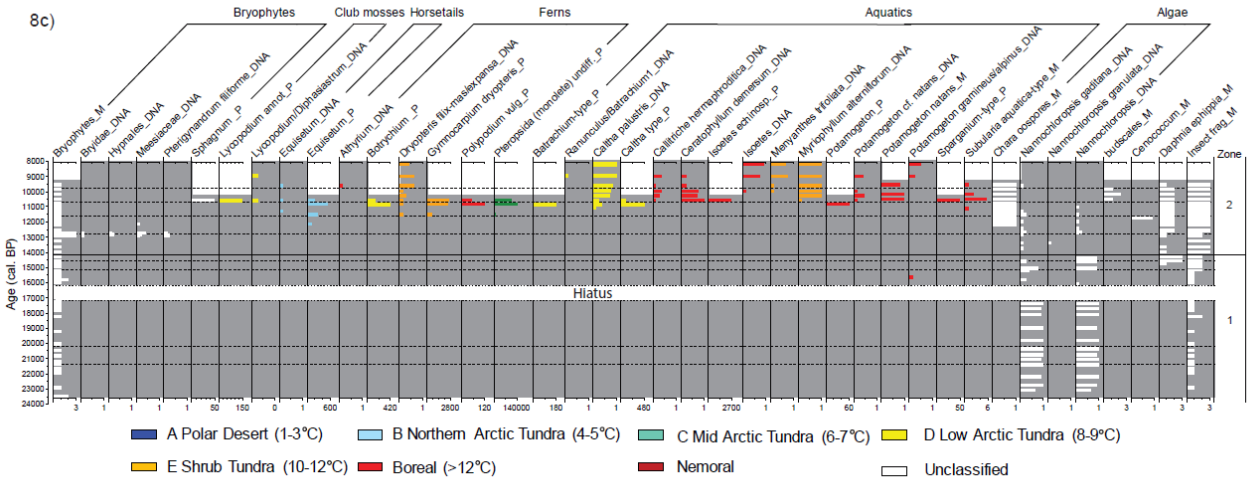
8c)
Bryophytes
Club mosses
Horsetails
Ferns
Aquatics
Algae
Bryophytes_M
Bryidae_DNA
Hypnales_DNA
Meesiaceae_DNA
Pleurozium schreberi_DNA
Sphagnum_P
Lycopodium annot_P
Lycopodium/Diphasiastrum_DNA
Equisetum_DNA
Equisetum_P
Athyrium_DNA
Botrychium_P
Dryopteris filix-mas/expansa_DNA
Gymnocarpium dryopteris_P
Polypodium vulg_P
Pteropsida (monolete) undiff_P
Batrachium-type_P
Ranunculus/Batrachium1_DNA
Caltha palustris_DNA
Caltha type_P
Callitriche hermaphroditica_DNA
Ceratophyllum demersum_DNA
Isoetes echinosp_P
Isoetes_DNA
Menyanthes trifoliata_DNA
Myriophyllum alterniflorum_DNA
Potamogeton_P
Potamogeton cf. natans_DNA
Potamogeton natans_M
Potamogeton gramineus/alpinus_DNA
Sparganium-type_P
Subularia aquatica-type_M
Chara oospores_M
Nannochloropsis gaditana_DNA
Nannochloropsis granulata_DNA
Nannochloropsis_DNA
cf.desicles_M
Cenococcum_M
Daphnia ephippia_M
Insect frag_M
Zone
Age (cal. BP)
Hiatus
A Polar Desert (1-3°C)
B Northern Arctic Tundra (4-5°C)
C Mid Arctic Tundra (6-7°C)
D Low Arctic Tundra (8-9°C)
E Shrub Tundra (10-12°C)
Boreal (>12°C)
Nemoral
Unclassified

1322